Automated Detection and Forecasting of COVID-19 using Deep Learning Techniques: A Review

Afshin Shoeibi, Marjane Khodatars, Mahboobeh Jafari, Navid Ghassemi, Delaram Sadeghi, Parisa Moridian, Ali Khadem, Roohallah Alizadehsani, *Member, IEEE,* Sadiq Hussain, Assef Zare, Zahra Alizadeh Sani, Fahime Khozeimeh, Saeid Nahavandi, *Fellow, IEEE,*, U. Rajendra Acharya, and Juan M. Gorriz

***Abstract*—Coronavirus, or COVID-19, is a hazardous disease that has endangered the health of many people around the world by directly affecting the lungs. COVID-19 is a medium-sized, coated virus with a single-stranded RNA, and also has one of the largest RNA genomes and is approximately 120 nm. The X-Ray and computed tomography (CT) imaging modalities are widely used to obtain a fast and accurate medical diagnosis. Identifying COVID-19 from these medical images is extremely challenging as it is time-consuming and prone to human errors. Hence, artificial intelligence (AI) methodologies can be used to obtain consistent high performance. Among the AI methods, deep learning (DL) networks have gained popularity recently compared to conventional machine learning (ML). Unlike ML, all stages of feature extraction, feature selection, and classification are accomplished automatically in DL models. In this paper, a complete survey of studies on the application of DL techniques for COVID-19 diagnostic and segmentation of lungs is discussed, concentrating on works that used X-Ray and CT images. Additionally, a review of papers on the forecasting of coronavirus prevalence in different parts of the world with DL is presented. Lastly, the challenges faced in the detection of COVID-19 using DL techniques and directions for future research are discussed.**

***Index Terms*—COVID-19, Diagnosis, Deep Learning, Classification, Segmentation, Forecasting.**

I. Introduction

The novel COVID-19 virus came to light in December 2019 in Wuhan Province, China, where it originated from animals and quickly spread around the world [1]. In January 2020, world health organization (WHO) announced the epidemic of COVID-19 as a threat to public health. In March 2020, it announced the Corona pandemic [2]. Coronaviruses include various types that mainly occur in animals. A type of Coronavirus, called SARS-CoV-2, is transmitted from bats to humans, threatening human health throughout the world [2]. SARS-CoV2 might stay alive on different surfaces from a few hours to several days. Clinical studies show that the incubation period of this virus is 1-14 days [2]. Recently, a new type of Coronavirus called Delta with a short incubation period has involved many people, and it has more dangerous complications [3].

The easiest way to transmit SARS-CoV-2 is through the air and physical contact, such as hand contact with an infected person [4]. The virus inserts itself into the lung cells through the respiratory system and replicates there, destroying these cells [5]. COVID-19 comprises an ribonucleic acid (RNA) and is very difficult to diagnose and treat due to its mutation characteristics [6]. The most common symptoms of SARS-CoV-2 include fever, cough, and shortness of breath, dizziness, headache, and muscle aches [2]. The virus is so perilous and can provoke the death of people with weakened immune systems [7]. Infectious disease specialists and physicians around the world are working to discover a treatment for the disease. COVID-19 is currently the leading cause of death for thousands of countries worldwide, including the USA, Spain, Italy, China, the United Kingdom, Iran, and others. Figure 1 shows the latest number of infected people worldwide due to COVID-19.

Currently, various methods have been proposed for fast diagnosis of the Coronavirus. Among the proposed methods, WHO has introduced the real-time reverse transcription polymerase chain reaction (PT-PCR) test as the gold standard of early diagnosis of COVID-19 [8]. Also, imaging methods like X-Ray, CT, and ultrasound are of significance for COVID-19 diagnosis.

According to the WHO, all diagnoses of corona disease must be confirmed by RT-PCR [9]. However, testing with RT-PCR is highly time-consuming, and this issue is risky for people with COVID-19. Hence, first, medical imaging is carried out for the primary detection of COVID-19, then the RT-PCR test is performed to aid the physicians in making final accurate detection. Two medical imaging techniques, X-ray, CT-scan, and ultrasound are employed to diagnose COVID-19 [10], [11].

X-ray modality is the first procedure to diagnose COVID-19, which has the advantage of being inexpensive and low-risk from radiation hazards to human health [12]. In the X-ray

A. Shoeibi, M. Khodatars, M. Jafari, D. Sadeghi, and P. Moridian are with the Data Science and Computational Intelligence Institute, University of Granada, Spain. (Corresponding author: Afshin Shoeibi, email: afshin.shoeibi@gmail.com).

N. Ghassemi is with the Computer Engineering Department, Ferdowsi University of Mashhad, Mashhad, Iran.

R. Alizadehsan, F. Khozeimeh, and S. Nahavandi. are with the Institute for Intelligent Systems Research and Innovation (IISRI), Deakin University, Victoria 3217, Australia.

A. Khadem is with the Faculty of Electrical Engineering, K. N. Toosi University of Technology, Tehran, Iran.

Sadiq Hussain is System Administrator at Dibrugarh University, Assam, India, 786004.

A. Zare is with Faculty of Electrical Engineering, Gonabad Branch, Islamic Azad University, Gonabad, Iran.

Z. Alizadeh Sani is with Rajaie Cardiovascular Medical and Research Center, and Iran University of Medical Sciences, Tehran, Iran.

U. R. Acharya is with the School of Mathematics, Physics and Computing, University of Southern Queensland, Springfield, Australia.

J. M. Gorriz is with the Data Science and Computational Intelligence Institute, University of Granada, Spain, and Dept. of Psychiatry. University of Cambridge, UK.

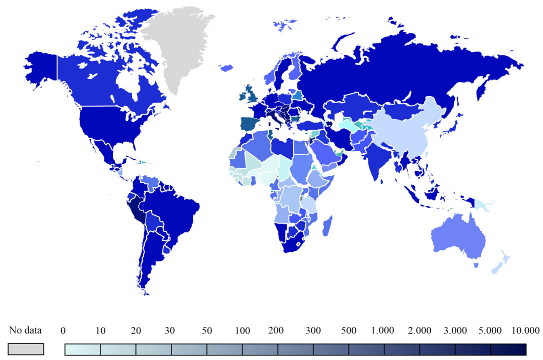

Fig. 1: The latest detailed statistics of COVID-19 infected people worldwide [9].

method, detecting COVID-19 is a relatively complicated task. In these images, the radiologist must attentively recognize the white spots that contain water and pus, which is very prolonged and problematic. A radiologist or specialist doctor may also mistakenly diagnose other diseases, such as pulmonary tuberculosis, as COVID-19 [13].

The X-ray procedure has a high error rate. CT modality has a higher contrast compared to X-Ray [11]. CT data of the patients suffering from SARS-CoV-2 demonstrate pulmonary parenchyma destruction, including interstitial inflammation and extensive consolidation accurately [14]. To detect the Coronavirus, numerous CT slices are recorded from each patient, which their analysis is challenging. To this end, the specialists try to remove the slices that do not contain important information.

Lung ultrasound is another Coronavirus diagnosis method [15]. Ultrasound plays an important role in diagnosing and treating the Coronavirus because it is not a radiative method. Also, ultrasound can assess different organs and systems, including the heart, arteries, and kidneys, that might have been damaged due to COVID-19 [15].

In recent years, applications of AI in medicine have led to a variety of studies aiming to diagnose varied diseases, including brain tumors from magnetic resonance (MR) images [16], [17], multiple types of brain disorders such from electroencephalography (EEG) [18], breast cancer from mammographic images [19], [20] and pulmonary diseases such as Covid-19 from X-Ray [10] and CT [11]. In the last decade, DL, a branch of ML, has changed the expectations in many applications of AI in data processing by reaching human-level accuracies [21] in many tasks, including medical image analysis [22].

In this paper, an overview of COVID-19 diagnostic approaches utilizing DL networks is presented. Section II explains the search strategy, and various DL models developed for COVID-19 detection are described in Section III. Section IV of the DL techniques used for the detection, segmentation, and prediction of COVID-19 patients. Section V discusses the reviewed papers on diagnosis, segmentation, and prediction of COVID-19 patients. Challenges in diagnosing, segmentation, and prediction of COVID-19 patients are provided in Section VI. Finally, the summary and future work are delineated in Section VII.

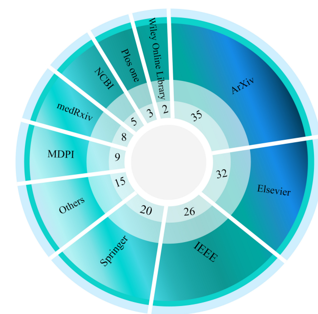

Fig. 2: Number of papers published on COVID-19 using DL techniques.

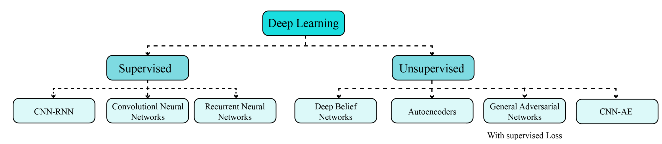

Fig. 3: Illustration of various DL methods used for COVID-19 detection.

II. Search Strategy

In this study, valid databases, including IEEE Xplore, ScienceDirect, SpringerLink, ACM, and ArXiv, have been used to search for Covid-19 papers. Moreover, a more detailed Google Scholar search is employed. The articles are selected using the keywords “COVID-19”, “Corona Virus”, “Deep Learning”, “Segmentation”, “Forecasting”, “Attention Deep Learning”, “Transformer Deep Learning”, “Data Fusion”, and “Graph Deep Learning”. The latest selection of papers is done with the mentioned keywords on September 19th, 2021. Figure 2 indicates the number of papers published or indexed by COVID-19 using DL techniques using various databases.

III. Deep Learning Techniques for COVID-19 Detection

Conventional machine learning and DL are the two main branches of AI, but DL is essentially a more advanced version of conventional ML. Various DL network architectures have been extensively used in research papers to diagnose the COVID-19 accurately using publicly available databases. Many of well-known DL architectures, such as convolutional neural networks (CNNs), recurrent neural networks (RNNs), Autoencoders (AEs), deep belief networks (DBNs), generative adversarial networks (GANs), and also some hybrid networks such as CNN-RNN and CNN-AE have been developed for automated detection of COVID-19. Figure 3 shows the subcategories of DL networks.

IV. Computer Aided Diagnosis System (CADS) for COVID-19 Detection

In prior research papers, many CADS have been developed applying DL methods on X-ray and CT images; these systems

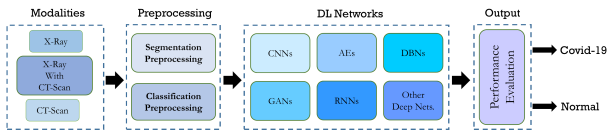

Fig. 4: Block diagram for COVID-19 detection using DL technique.

TABLE I: Public databases used for COVID-19 detection.

Dataset	Modality	Link
J. P. Cohen's GitHub [26]	X-ray and CT	https://github.com/ieee8023/covid-chestxray-dataset
European Society of Radiology	X-ray and CT	https://www.eurorad.org/advanced-search?search=COVID
SIRM	X-ray and CT	https://www.sirm.org/category/senza-categoria/covid-19
BSTI	X-ray and CT	https://www.bsti.org.uk/covid-19-resources
UCSD-AI4H [27]	CT	https://github.com/UCSD-AI4H/COVID-CT
MedSeg	CT	http://medicalsegmentation.com/covid19
Kaggle	X-ray and CT	https://www.kaggle.com/datasets?search=covid
Point-of-Care Ultrasound (POCUS) [28]	Lung Ultrasound Images and Videos	https://github.com/jannisborn/covid19_pocus_ultrasound
Actualmed COVID-19 Chest X-ray Dataset Initiative	X-ray	https://github.com/agchung/Actualmed-COVID-chestxray-dataset
COVID-19 Chest X-ray Dataset Initiative	X-ray	https://github.com/agchung/Figure1-COVID-chestxray-dataset
Georgia State University's Panacea Lab [29]	Twitter Chatter Dataset	https://github.com/thepanacealab/covid19_twitter
Twitter COVID-19 CXR dataset	X-ray	https://twitter.com/ChestImaging
COVID-19 [30]	CT	https://github.com/KevinHuRunWen/COVID-19
COVIDx [31]	X-ray	https://github.com/lindawangg/COVID-Net

can be categorized by their application into two categories: (i) classification and (ii) segmentation. In classification-based CADS, the main objective is to identify COVID-19 patients, which involves the process of extracting and selecting the most informative features and classifying using DL. However, in the second type, an image of an infected person is given to the system for segmentation of an area of interest. Manual segmentation of medical images takes considerable time; thus, applying machine learning models is crucially paramount. Among the most important segmentation models, the several types of fuzzy clustering methods [23], [24] and DL ones such as U-Net [25] can be denoted. In the CADS, with the segmentation approach, patients' CT-Scan images and their manual segments labeled by doctors are fed to the DL network. Then, during the training process, the DL network is trained on manual segments to segment raw input images. The components of DL-based CADS for COVID-19 detection are shown in Figure 4. In the following section, we will first mention the important data available for COVID-19; then, the DL methods used in the review research are introduced.

A. Public Databases used for COVID-19 Detection and Forecasting

Several public databases (X-ray and CT images) are available for the detection and segmentation of COVID-19, some of them are listed in Table I. Also, the datasets related to predicting the COVID-19 spread in leading countries of the world are shown in Table II.

B. Deep Learning Methods

This section is devoted to describing the methods applied in papers briefly. First, well-known network structures for both classification and segmentation are discussed; then, models which are applied for forecasting are explained and lastly, new trends and state-of-the-art methods are presented.

TABLE II: Public COVID-19 forecasting databases used for forecasting.

Dataset	Modality	Link
China CDC Weekly	Daily Number of Cases in China	http://weekly.chinacdc.cn/news/TrackingtheEpidemic.htm
The Ministry of Health and Family Welfare (Government of India)	Daily Number of Cases in India	https://www.mohfw.gov.in
Johns Hopkins University	Tracking COVID-19 Spread	https://systems.jhu.edu
WHO COVID-19 Dashboard	Global Statistics	https://covid19.who.int
U.S. CDC	Daily Number of Cases in U.S.	https://www.cdc.gov/coronavirus/2019-ncov/cases-updates/cases-in-us.html https://www.cdc.gov/coronavirus/2019-ncov/covid-data/data-visualization.htm
Worldometer	Global Collection	https://www.worldometers.info/coronavirus
Open Source COVID-19	Global Collection	http://open-source-covid-19.weileizeng.com
Painel Coronavírus	Daily Number of Cases in Brazil	https://covid.saude.gov.br
GOV.UK	Daily Number of Cases in UK	https://coronavirus.data.gov.uk
Ministero della Salute	Daily Number of Cases in Italy	http://www.salute.gov.it/portale/nuovocoronavirus/homeNuovoCoronavirus.jsp?lingua=english
Ministry of health	Daily Number of Cases in Spain	https://www.mscbs.gob.es/profesionales/saludPublica/ccayes/alertasActual/nCov-China/situacionActual.htm https://cnecovid.isciii.es/covid19

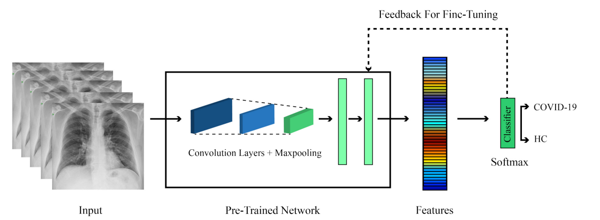

Fig. 5: Overall diagram of pre-trained methods.

1) Classification Models: CNNS AND PRE-TRAINED MODELS

The primary issue in training the deep models is the concern of overfitting that occurs from the gap between the limited number of training samples and a large number of learnable parameters. Convolutional networks try to overcome this by using convolutional layers [32]. CNNs require minimal pre-processing by considering the 2-dimensional (2D) images as input, and hence it is designed to retain and utilize the structural information among neighboring pixels or voxels. A differentiable function is utilized to transform one volume of actions by each layer to the other as it is a sequence of layers structurally.

While convolutional layers work as some sort of workaround for the issues of deep neural networks, training CNNs properly still needs a massive amount of data, and also designing their structure is itself a time-consuming process. To overcome these problems, researchers usually use a pre-trained version of well-known network architecture. Figure 5 shows how the pre-trained networks are used; also, some of the most used network architectures are : AlexNet [33], Visual Geometry Group (VGG) network [34], GoogLeNet [35], ResNet [36], DenseNet [37], and, SqueezeNet [38].

2) Generative Adversarial Networks (GAN): A primary problem in training deep models is limits in dataset size. Using generative models for data augmentation is one solution to this issue. Due to the high quality of generated data, GANs have attracted attention in the medical imaging community [39]. The basic idea in training a GAN is a simple minimax game, in which one network tries to distinguish between real data and generates one, and the other tries to create data undistinguishable by the first network [40], therefor creating images similar to real data.

3) Segmentation Models: A wide variety of DL models have been developed for the segmentation of the lung region to detect COVID-19 in patients accurately. Among these models, FCN network [41], SegNet [42], U-Net [25], and Res2Net [43]

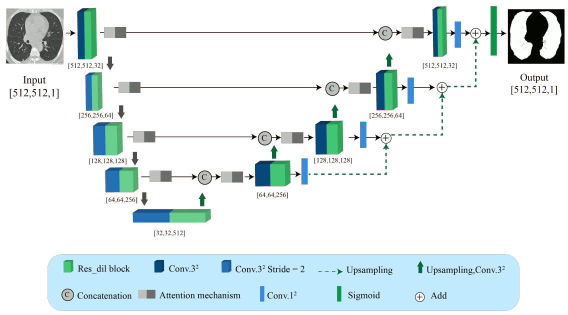

Fig. 6: A typical U-Net architecture used to segment the lung in COVID-19 patients [44].

DL models are widely used for the segmentation of lungs. In this section, some of these models are briefly discussed.

SEGNET

Generally, in segmentation techniques, a network created for classification is chosen, and the FC layers of that network are removed; the resulting network is called the encoder network. Then a decoder is created to transform these low-resolution maps to the original resolution. In SegNet [42], the decoder is created such that for each down-sampling layer in the encoding section, an up-sampling layer is positioned in the decoder. These layers, unlike the deconvolution layers of FCN networks, are not capable of learning, and the values are placed at the locations from which the corresponding max-pooling layer is extracted, and the rest of the output cells become zero.

U-NET

The U-Net network [25], like SegNet, consists of the identical numbers of pooling and up-sampling layers, but the network utilizes trainable deconvolution layers. Also, in this network, there is a corresponding skip connection between the up-sampling and down-sampling layers. Figure 6 shows a general form of U-Net architecture used to segment the lung in COVID-19 patients.

4) Forecasting Models: RECURRENT NEURAL NETWORK(RNN)

A feed-forward neural network is extended to create RNN, aiming to capture the long term dependencies and features from the sequential and time-series data. The most commonly used RNN is the long-short term memory (LSTM), which composed of a memory cell, a forget cell, the input gate, and output gate. These gates make the decision that which information needs to be remembered or discarded from the memory cell and also organizes the activation signals from different sources.

LSTM decides whether to keep or remove the memory by using these gates; also, unlike vanilla RNN, LSTM can preserve the potential long term dependencies. One LSTM variant is Gated Recurrent Unit (GRU) [45], which integrates the forget and input gates into a single update gate and combines the memory cell state and the hidden state into one state. Update gate makes a decision on the amount of information to be added or discarded, and the reset gate decides on how much earlier information is to be forgotten. This technique makes GRU simpler than LSTM.

5) Advanced AI methods for Diagnosis of COVID-19: DEEP ATTENTION LEARNING

The DL methods based on attention mechanisms have attracted attention recently [46]. The models based on attention mechanism are concentrated on a subset of inputs (focus on certain parts of the input) that contain information regarding the tasks [46]. Recently, attention models have been used in various applications, including classification, segmentation, and diagnosis of COVID-19. In [46], a DL model based on attention with the attention module of VGG-16 has been used to classify COVID-19 using X-Ray images.

DEEP TRANSFORMER LEARNING

Transformer models are another type of DL method, and some of their techniques include spatial transformer networks, graph transformer networks, recurrent spatial transformer networks, and Polar transformer networks. In [47], COVID-19 has been diagnosed using ultrasound data based on the vision transformer (ViT) model.

DEEP FUSION TECHNIQUES

With the emergence of DL models, it has been tried to combine data fusion techniques and DL networks with medical objectives. In [48], CT data have been extracted using four CNNs to classify Corona data. Then, feature integration and ranking techniques have been used to obtain effective features. Finally, the SVM classifier has been used.

GRAPH DEEP LEARNING

The graph models based on DL are another class of new DL techniques that have been recently used in detecting the coronavirus. In [49], first, a 3D-CNN has been used to extract features from CT images. Then, a COVID-19 graph in GCN has been designed based on the features. Finally, these three DL models are combined to detect the COVID-19.

V. DISCUSSION

The main focus of this work is to review the research papers that have worked on DL models for detection, segmentation of the lungs and also forecasting the spread of the COVID-19. The summary of works done on classification, segmentation, and forecasting are presented in Tables III, IV, and V, respectively. Figure 7 depicts the total number of investigations conducted in the field of classification, segmentation, and forecasting of COVID-19 using DL models. It can be noted from the figure that most works have been done on the detection of COVID-19 patients, and the least works are done on forecasting due to the shortage of available public databases.

TABLE III: Summary of state-of-art DL techniques used for the automated detection of COVID-19 patients.

Work	Dataset	Modalities	Number of Cases	Preprocessing	DNN toolbox	DNN	Number of Layers	Classifier	Post Processing	K-Fold	Performance Criteria (%)
[50]	COVIDx	X-ray	45 COVID-19, 1203 Normal, 931 Bacterial Pneumonia, 660 Viral Pneumonia Patients	Data Augmentation (DA), Rescaling, Normalizing	Fastai Library	COVID-ResNet (ResNet-50)	Modified Version	Softmax	NA	NA	Acc=96.23 Sen=100 Pre=100 F1-Score=100
[51]	Combination of Different Datasets	X-ray	50 COVID-19, 50 Normal Images	Rescaling	NA	ResNet50	Modified Version	Softmax	NA	5	Acc=98 Recall=96 Spe=100
[33]	Combination of Different Datasets	X-ray, CT-Scan	85 COVID-19 X-ray, 203 COVID-19 CT-scan, 85 Normal X-ray, 153 Normal CT-scan	Cropping, resizing	NA	AlexNet	Modified Version	Softmax	NA	NA	Acc=98 Sen=100 Spe=96
[52]	Cohen's GitHub	X-ray	25 COVID-19, 25 Normal Cases	Rescaling	Keras with Tensor-Flow2 Backend	COVIDX-Net (VGG19, DenseNet201)	Standard Version	Softmax	NA	NA	Acc=90 Pre=83 F1-Score=91
[53]	Combination of Different Datasets	X-ray	70 COVID-19 subjects, 1008 Pneumonia Subjects	Rescaling, DA	NA	ResNet-18	Standard Version + 8	Sigmoid	Grad-CAM	NA	Sen=96 Spe=70.65 AUC=95.18
[54]	BIMCV, COVIDx	X-ray	8851 HC, 6045 Pneumonia, 3323 COVID-19	Filtering	PyTorch	Fus-ResNet50	Modified ResNet50	Softmax	–	5	Acc=95.57 Pre=99 F1-Score=99
[55]	COVIDx	X-ray	76 COVID-19, 1583 Normal, 4290 Pneumonia Cases	DA, RGB format, Normalizing	MATLAB	COVIDiagnosis-Net	Standard Version	Decision-Making System	Class Activation Mapping Visualization	NA	Acc=98.3 Spe=99.13 F1-Score=98.3
[56]	Combination of Different Datasets	X-ray	68 COVID-19, 1583 Normal, 2786 Bacterial Pneumonia, 1504 Viral Pneumonia Images	Resizing, Standardizing, DA	Keras	ResNet50-V2	Modified Version	Softmax	saliency Maps Visualization, Different Gradient Methods	NA	Predictive Entropy=99.68 BALD=88.73
[57]	Combination of Different Datasets	X-ray	295 COVID-19, 65 Normal, 98 Pneumonia Images	Fuzzy Color Method, Image Stacking Technique	MATLAB	MobileNetV2 SqueezeNet	Standard Version	SMO, SVM	Social Mimic Optimization Method	5	Acc=99.27
[58]	Clinical	CT-Scan	368 COVID-19 Patients, 127 Patients with Other Pneumonia	Segmentation, Rescaling, Multi-view Fusion	Keras	ResNet50	Modified Version	Dense Layer	NA	NA	Acc=76 Sen=81.1 Spe=61.5
[10]	Clinical	X-ray	3270 HC, 1281 COVID-19 Infected, and 4657 Pneumonia x-ray images	Resizing, Normalization	NA	Fused-DenseNet-Tiny	Modified DenseNet	Softmax	–	–	Acc=97.99 Pre=98.38 F1-Score=98.26
[59]	Clinical	CT-Scan	108 COVID-19, 86 Non-COVID-19 Patients	Different Methods	NA	ResNet-101, Xception	Standard Version	Softmax	NA	NA	Sen=98.04 Spe=100 Acc=99.02
[60]	Combination of Different Datasets	X-ray	105 COVID-19 ,11 SARS, 80 Normal Samples	DA, Histogram, Feature Extraction using AlexNet, PCA, K-means	MATLAB	DeTraC (ResNet18)	Standard Version	Softmax	Composition Phase	NA	Acc=95.12 Sen=97.91 Spe=91.87
[61]	RYDLS-20	X-ray	90 COVID-19, 10 MERS, 11 SARS, 10 Varicella, 12 Streptococcus, 11 Pneumocystis Samples	Different Features, Early Fusion, Late Fusion, Different Resampling Algorithms	NA	Inception-V3	Standard Version	MLP Clus-HMC Framework	Friedman Statistical Test for Ranking	NA	F1-Score=83.33 F1-Score=88.89
[62]	Pneumonia Dataset	X-ray	624 Images in 2 Categories: Normal and Pneumonia	GAN	MATLAB	ResNet18	Standard Version	Softmax	NA	NA	Acc=99 Pre=98.97 F1-Score=98.97
[63]	Different Datasets	X-ray	3111 HC, 1979 COVID-19	Converting RGB to Gay, Filtering, Segmentation, Normalization	NA	Feature Fusion based on VGG19	VGG19	Softmax	–	5	Acc=98.36
[64]	COVIDx	X-ray	NA	NA	NA	COVID-CAPS	9	Capsule Layer	NA	NA	Acc=95.7 Sen=90 Spe=95.8
[65]	Combination of Different Datasets	X-ray	284 Covid-19, 310 Normal, 330 Pneumonia Bacterial, 327 Pneumonia Viral Images	Rescaling	Keras with Tensor-Flow Backend	CoroNet	Modified Version	Softmax	NA	NA	Acc=89.5 Pre=97 F1-Score=98
[66]	Kaggle	X-ray	5,863 X-Ray Images in Two Classes Normal and Pneumonia, 145 Chest X-ray Images of COVID-19	Rescaling	Keras with Tensor-Flow Backend	DenseNet169	Standard Version	Softmax	NA	NA	Avg Acc=95.72
[67]	COVIDx	X-ray	13; 800 Images from 13; 645 Individuals	Intensity Normalization, DA	Keras with Tensor-Flow Backend	EfficientNet B3	50	Softmax	Activation Map Visualization	NA	Acc=93.9 Sen=96.8
[68]	3 Different COVIDx Datasets	X-ray	Different Number of Cases	Different Methods	Keras with Tensor-Flow Backend	DenseNet-161	Modified Version	Softmax	Grad-CAM, Grad-CAM++, LRP Visualizations	5	Pre=94 Recall=95 F1-Score=94.5
[69]	Clinical	X-ray	27 Normal, 220 COVID-19, 11 SARS and 15 Pneumocystis Images	Filtering	Keras, TensorFlow	Feature Fusion (FM-HCF-DLF model)	Modified Inception v3	Sigmoid	–	10	Acc=94.08 Sen=93.61 Spe=94.56
[70]	Combination of Different Datasets	X-ray	99 COVID-19 Cases From the COVID19 Chest X-ray Dataset, 207 Images From Both Dataset	Balancing dataset, DA	Keras	GSA-DenseNet121-COVID-19	Modified Version	Softmax	NA	NA	Acc=98 Pre=98 F1-Score=98
[38]	COVID-Xray-5k Dataset	X-ray	536 COVID-19 Images, 5000 Non-COVID19	DA, Down Sampling	PyTorch	SqueezeNet	Standard Version	Softmax	NA	NA	Sen=97.5 Spec=97.8
[71]	Combination of Different Datasets	X-ray	207 COVID-19 Images, 5,863 Non-COVID-19 Images	DA	NA	DenseNet-161	Modified Version	Softmax	NA	NA	Acc=99 Pre=100 F1-Score=99
[72]	Clinical	CT Scan	397 HC, 349 COVID-19	Transforming CT Images to 2D image, Resizing	NA	Fusion FDEP-FGN and RFINCA	Different Layers	Sigmoid	–	10	Acc=95.84
[11]	Clinical	CT Scan	2373 COVID- 19, 2890 Pneumonia, 3193 Tuberculosis, 3038 HC	Different Methods	NA	Ensemble the PreTrain Models	DenseNet201, ResNet152V2, and VGG16	Softmax	–	–	Acc=98.83 Sen=98.83 Spe=98.82
[73]	Combination of Different Datasets	X-ray	225 COVID-19 Images, 108,948 Frontal View Images From 32,717 Unique Patients	DA	Keras with Tensor-Flow Backend	CN	12	FCMLP	Grad-CAM	5	Acc=95.3

[74]	Combination of Different Datasets	X-ray	180 COVID-19 Images, 6054 Pneumonia, 8851 Normal	NA	Keras	Concatenation of Xception and ResNet50V2	Modified Version	Softmax	NA	5	Acc=99.56
[75]	Combination of Different Datasets	X-ray	NA	Different Methods	PyTorch	COVID-DA	Modified Version	NA	Grad-CAM	NA	Pre=98.15 AUC=98.5
[76]	Combination of Different Datasets	X-ray	NA	Cropping, CLAHE Method, Resizing, DA	NA	CovIDNet	15	Softmax	NA	NA	Acc=98.4 Sen=100 Spe=96.97
[77]	COVIDx	X-Ray	6053 Pneumonia, 8851 Normal, 573 COVID-19 Cases Images	–	TensorFlow	EDL-COVID	COVID-Net	WAE Approach	–	–	Acc=95 Sen=96
[78]	Clinical	CT-Scan	88 COVID-19 Patients, 100 Bacteria Pneumonia Patients, 86 Healthy Persons	Different Methods	OpenCV	DRE-Net (ResNet-50 Backbone)	Modified Version	Aggregation	Visualization	NA	Acc=94 AUC=99 Pre=96
[79]	Clinical	CT Scan	400 COVID-19 Patients	Segmentation, Resizing, Cropping, Normalization	PyTorch	Deep Fusion Architecture	ResNet10 and Quantitative 3D Radiomics Model	Ensemble Learning	Grad-CAM	5	Acc=83.6 Sens=75 Spec=84.2
[80]	Combination of Different Datasets	X-Ray, CT-Scan	200 of COVID-19, 200 Healthy, 200 Bacterial Pneumonia 200 Viral Pneumonia	NA	Caffe	ResNet101	Standard Version	Softmax	NA	10	Acc=98.75 Spe=97.50 Sen=100 Pre=96.43
[81]	COVIDx	X-Ray	13975 CXR Images from 13870 Patients	–	PyTorch	RCoNet	4 Module	–	Uncertainty Estimation	–	Acc=97.89 Sen=97.33 Spec=98.24
[14]	COVID-19 X-Ray Dataset	X-Ray	5,863 X-Rays normal or Pneumonia	DA	–	ResNet-50	Standard Version	ASSOA C + MLP	–	–	Acc=99.7
[82]	Combination of Different Datasets	X-ray	314 COVID-19	Segmentation using U-Net, Standard Preprocessing, Weakly-Labeled DA	Keras with Tensor-Flow Backend	VGG-16	Standard Version	Softmax	Grad-CAM	NA	Acc=99.26
[83]	Clinical	CT-Scan	109 COVID-19, 201 Non-COVID-19	Standard Preprocessing, Generating Pseudo-Infection Anomalies using BCDU-Net	NA	CovidCTNet	19	Softmax	NA	NA	Acc=90 Sen=83 Spe=92.85
[84]	Kaggle Data Repository	X-ray	150 COVID-19	Filtering, Segmentation using Thresholding	NA	CNN	11	Softmax	NA	NA	Acc=93
[85]	Combination of Different Datasets	CT-Scan	521 COVID-19, 521 Non-COVID-19	DA, Random Cropping Operation	NA	CNN with ShuffleNetV2 as the backbone	Standard Version	Linear Layer	NA	NA	Acc=91.21 Sen=90.52 Spe=91.58
[86]	Different Datasets	X-Ray	142 COVID-19, 141 Normal, 141 Pneumonia	Resizing, Shuffling, Normalization	Keras with Tensor-Flow Backend	GRU-CNN	7	Softmax	GRAD-CAM	NA	Pre=100 Re=100 F1-Score=100
[87]	Different Datasets	CT-Scan	349 COVID-19, 397 Non-COVID-19	DA, Self-Trans Method	PyTorch	DenseNet-169	Standard Version	Softmax	Grad-CAM	NA	Acc=86 F1-Score=85 AUC=94
[88]	Clinical	CT-Scan	3389 COVID-19, 1593 Non-COVID-19	Standard Preprocessing, VB-Net Toolkit for Segmentation and Lung Mask Generation	PyTorch	3D ResNet34 with Online Attention Module	Modified Version	Ensemble Learning	Grad-CAM	5	Acc=87.5 Sen=86.9 Spe=90.1 AUC=94.4
[89]	COVIDx	X-ray	238 COVID-19, 14896 Non-COVID-19	DA	TensorFlow	DenseNet-121	Modified Version	Softmax	Grad-CAM	10	Acc=96.4 Pre=96 Recall=96
[90]	Clinical	CT-Scan	146 COVID-19, 149 Non-COVID-19	DA	PyTorch	DenseNet	Standard Version	Softmax	CAM	NA	Acc=92 Sen=97 Spe=87
[91]	Combination of Different Datasets	X-ray	158 COVID-19, 158 Non-COVID-19	NA	MATLAB	ResNet50	Standard Version	SVM	NA	NA	Acc=95.38 Sen=97.29 Spe=93.47
[92]	Combination of Different Datasets	X-ray	455 COVID-19 Images, 2109 Non-COVID-19 Images	Rescaling, DA	Keras with Tensor-Flow Backend	MobileNet V2	Modified Version	NA	NA	10	Acc=99.18 Sen=97.36 Spe=99.42
[93]	Combination of Different Datasets	X-ray	403 COVID-19 Images, 721 Non-COVID-19 Images	Resizing, Normalizing, DA using CovidGAN Based AC-GAN	Keras	VGG16	Standard Version	Softmax	PCA Visualization	NA	Acc=95 Sen=90 Spe=97
[94]	Different Datasets	CT-Scan	558 COVID-19	2D CNNs for the Segmentation	pyTorch	COPLE-Net	Proposed Architecture	Softmax	Noise-Robust Loss Functions	–	Dice=80.72
[35]	Combination of Different Datasets	X-ray	69 COVID-19 Images, 79 Normal, 79 Pneumonia Bacterial, 79 Pneumonia Viruses	DA using GAN	MATLAB	GoogLeNet	Standard Version	Softmax	NA	NA	Acc=100 Pre=100
[95]	Combination of Different Datasets	CT-Scan	1118 COVID-19 Images, 96 Pneumonia Images, 107 Healthy Images	Different Methods	MATLAB	CNN (Feature Extraction)	12	LSTM	NA	NA	Acc=99.68
[15]	Clinical	Ultrasound	69 Covid-19, 66 HC, 50 Bacterial Pneumonia Videos	Cropping	Keras with Tensor-Flow Backend	VGG16-LSTM	–	Softmax	–	5	Acc=93 Sen=97
[96]	Combination of Different Datasets	X-ray	224 Covid-19 cases, 504 Healthy Cases, 400 Bacteria, 314 Viral Pneumonia	Resizing	NA	MobileNet	Modified Version	NA	NA	NA	Acc=96.78 Sen=98.66 Spe=96.46
[97]	Combination of Different Datasets	X-ray	219 COVID-19 Images, 1341 Normal Lung Images, 1345 Viral Pneumonia Images	Manually editing, Reshaping, DA	PyTorch	CheXNet (DenseNet121 Backbone)	Modified Version	Sigmoid	Heatmaps Generation using LRP	NA	Acc=98.3 Pre=98.3 F1-score=98.3
[98]	Different Datasets	X-ray	49 COVID-19 Images, 88,079 Non-COVID-19 Images	Standard Preprocessing	TorchXRayVision Library	DenseNet	Modified Version	Sigmoid, LR	t-SNE, Saliency Maps	NA	MAE=1.14

[99]	Combination of Different Datasets	X-ray	190 COVID-19, 1345 Viral Pneumonia, and 1341 Normal Chest X-ray Images	Resizing, Normalization, DA	MATLAB	SqueezeNet	Modified Version	Softmax	NA	5	Acc=98.3 Sen=96.7 Spe=100 Pre=100
[100]	COVID-CT-Dataset	CT-Scan	345 COVID-19, 397 Non COVID-19	Resizing, DA using CGAN, Normalizing	TensorFlow	ResNet50	Modified Version	Softmax	NA	NA	Acc=82.91 Sen=80.85 Spe=91.43
[101]	Combination of Different Datasets	X-ray	180 COVID-19 cases, 6054 Pneumonia Cases, 8851 Normal Cases	DA	Keras	Concatenation of the Xception and ResNet50V2	Modified Version	Softmax	NA	5	Acc=91.4
[102]	Kaggle	X-ray	70 COVID-19 and 80 Normal Images	Resizing, DA	NA	VGG16, VGG19	Modified Version	Softmax	NA	NA	Acc=97 Sen=100 Spe=94
[103]	Combination of Different Datasets	X-ray	215 COVID-19, 6045 CAP, 8851 Normal Images	DA	PyTorch	Different PreTrain Deep Networks	Modified Version	Softmax	NA	NA	Ensemble of Models: Acc=89.4
[104]	Combination of Different Datasets	X-ray	69 COVID-19, 79 Normal, 79 Pneumonia Bacterial, 79 Pneumonia Virus Images	Resizing, Neutrosophic Image Domain Conversion, Normalizing	MATLAB	GoogLeNet	Standard Version	Softmax	NA	NA	Acc=73.12
[105]	Combination of Different Datasets	X-ray, CT-scan	117 X-ray and 20 CT Scan of COVID-19, 117 Healthy X-ray Images, 20 Healthy CT Scan Images	Resizing, Normalizing	Keras with Tensor-Flow Backend	DenseNet121	Standard Version	Bagging Tree	Web-Based Application	10	Acc=99 Pre=96
[106]	Combination of Different Datasets	X-ray	181 COVID-19 Images, 364 Healthy Images	Normalizing, Resizing	NA	VGG-19	Modified Version	Softmax	NA	NA	Acc=96.3
[107]	Clinical	CT-Scan	151 COVID-19 Patient, 498 Non-COVID-19 Patient	Resizing, Padding, DA	NA	3D-CNN	15	Softmax	Visual Interpretation by Two Experienced Radiologists	NA	AUC=70
[108]	Public Datasets & Private Datasets	CT-Scan	1,684 COVID-19 Patient, 1,055 Pneumonia, 914 Normal Patients	Resizing	NA	Inception V1	Modified Version	Softmax	Interpretation by 6 Radiologists, t-SNE Method	10	Acc=95.78 AUC=99.4
[109]	Combination of Different Datasets	CT-Scan	413 COVID-19 Images and 439 Normal or Pneumonia Infected Patients' Images	ResNet50 (Feature Extraction)	NA	CNN	14	Softmax	NA	10	Acc=93.01 Spe=94.77 Sen=91.45
[110]	Combination of Different Datasets	X-ray	142 COVID-19 Images, 142 Normal Images	Resizing, DA	NA	NCOVnet (VGG-16)	Modified Version	Softmax	NA	NA	Acc=97.62 Sen=97.62 Spe=78.57
[111]	Combination of Different Datasets	X-ray	326 COVID_19 Images, 984 Non-COVID-19 Images	Manual Annotation, Data Balancing and Augmentation Strategies, Normalizing, Resizing	NA	CNN with YOLO Predictor	54	Tensor of Prediction (ToP)	NA	5	Acc=97.40 Spe=99.056 Sen=85.15
[112]	Combination of Different Datasets	X-ray	250 COVID-19, 2,753 Other Pulmonary Diseases, 3,520 Healthy Images	Resizing, DA	NA	VGG-16	Modified Version	Softmax	Grad-CAM	NA	Acc=97 Sen=87 Spe=94
[113]	Combination of Different Datasets	X-ray	179 COVID-19, 179 Pneumonia, 179 Normal Images	Create a Noisy Snapshot Dataset	PyTorch	DenseNet-121, ShuffleNetV2, MobileNetV2	Modified/ Standard Versions	NA	t-SNE, GRAD-CAM	NA	Acc=84.3 AUROC=94
[114]	Another Reference	CT-Scan	73 Patients with COVID-19	MODE Algorithm for Hyper-Parameter Tuning	MATLAB	CNN	7	NA	NA	20	Acc=92 Sen=90 Spe=90
[115]	POCUS	Ultrasound	1283 COVID-19, 731 Bacterial Pneumonia, 1312 HC	Cropping, Resizing	Keras	InceptionV3	Standard Architecture	Softmax	–	5	Acc=89.1 Pre=90.1 F1-Score=88
[116]	Clinical	CT-Scan	98 COVID-19 Patients, 103 Non-COVID-19 Patients	Visual Inspection	Google Colaboratory	BigBiGAN	NA	Linear Classifier	NA	NA	AUC=97.2 Sen=92 Spe=91
[117]	Clinical	Ultrasound	1530 LUS Scans with 287,549 Frames	Cropping, Resizing, Filtering, Smoothing	TensorFlow	Two-Stream Inflated 3D Conv-Net	–	Softmax	–	5	Acc=90 Pre=95
[118]	UCSD-AI4H Datasets	CT-Scan	349 Patients with Confirmed COVID and 397 Healthy Subjects	Resizing, Normalizing	Keras with Tensor-Flow Backed	DenseNet121	Standard Version	Nu-SVM	Web based CAD Implementation with Flask RESTful	10	Acc=90.61 Recall=90.80 Pre=89.76
[119]	Different Datasets	X-ray	219 COVID-19, 1341 Normal, 1345 Viral Pneumonia Images	Resizing, Normalizing, DA	PyTorch, Keras with Tensor-Flow Backend	DenseNet-201	Modified Version	Sigmoid	LRP	NA	Acc=99.4 Pre=99.5 F1-Score=99.4
[120]	Different Datasets	X-ray	536 COVID-19 Images, 619 Viral Pneumonia, and 668 Normal Images	White Balance Algorithm, CLAHE, Normalizing, Resizing	Keras with Tensor-Flow Backend	COVIDLite	38	Softmax	t-SNE,S Maps, Grad-CAM, LIME	5	Binary Acc=99.58 Multi-Class Acc=96.43
[121]	POCUS	Ultrasound	1103 Images (678 Covid-19, 277 Pneumonia, 182 Healthy)	Cropping Videos to Images	TensorFlow	Mini Covid-Net	–	Softmax	–	5	Acc=83.2 Sen=92 Spe=71
[122]	Combination of Different Datasets	X-ray	X-rays of 327 Patients	Resizing, DA, Normalizing	NA	VGG16	Modified Version	Softmax	NA	5	Acc=84.1
[123]	COVIDx	X-ray	183 COVID-19 Images, 5551 Pneumonia Images, 8066 Normal Images	NA	NA	COVIDNet-CXR Small and COVID-Net-CXR Large	Standard Version	NA	UAPs using FGSM	NA	Acc=92.6 Avg Acc=94.4
[124]	Combination of Different Datasets	X-ray	127 COVID-19 Images, 127 Pneumonia Images, 127 Healthy Images	NA	MATLAB	ResNet50	Standard Version	SVM	NA	NA	Acc=95.33 Sen=95.33
[125]	Combination of Different Datasets	X-ray	738 Images of COVID-19, 5000 Normal, 4600 Images of CAP	DA, Normalization, Resizing, CLAHE, BEASF	NA	CNN	8	NA	Grad-CAM, LIME	NA	Acc=98.68 AUC=99.84
[126]	Clinical	Ultrasound	2908 Frames from 450 Hospitalized Patients	Cropping, DA	MATLAB	ResNet-50	Standard Architecture	Softmax	–	–	Acc=97.93

TABLE IV: Summary of DL segmentation methods used for COVID-19 detection.

Work	Dataset	Modalities	Number of Cases	Preprocessing	DNN toolbox	DNN	Number of Layers	Classifier	Post Processing	K-Fold	Performance Criteria (%)
[127]	Different Clinical Datasets	CT-Scan	157 International Patients	Detect and Measure Nodules, Lung Crop using U-net, DA	NA	ResNet50	Standard	Corona Score Computation	Grad-Cam, 3D Visualization	NA	AUC=99.6 Sen=98.2 Spe=92.2
[128]	Clinical	CT-Scan	549 COVID-19 Patients	HITL Strategy	NA	VB-Net	8 Block	NA	Quantitative Metrics Measurements	NA	DSC=91.6 Mean POI Estimation Error=0.3
[129]	Combination of Different Datasets	CT-Scan	610 COVID-19 Images, 695 Non-COVID-19 Images	Resizing, DA	PyTorch	DenseNet-169 + ASPP Layer	Standard	NA	NA	NA	AUC=94.8 Acc=83
[130]	Different Datasets	CT-Scan	110 Axial CT-Scan Images From 60 Patients	Resizing, Grey Scaling (GL), DA	NA	Residual Attention U-Net	9 ResNeXt blocks+14 Layers	Sigmoid	Visualization	10	Acc=89 Pre=95 DSC=94
[131]	Different Datasets	CT-Scan	Different Number of Cases	Lung Segmentation using U-net with a VGG-16 Based Encoder, DA	NA	ResNet50	Standard	Sigmoid	GradCam, Combine the Fine Grain Maps to Create 3D Localization Maps, K-Means	NA	AUC=99.4 Sen=94 Spec=98
[43]	COVID-CS Dataset	CT-Scan	144,167 CT-Scan Images of 400 COVID-19 Patients and 350 Uninfected Cases	DA, Segmentation using Encoder-Decoder Model	NA	Res2Net	Standard	Softmax	Visualization of Activation Mapping	NA	Avg Sen=95 Spe=93
[132]	Italian Society of Medical and Interventional Radiology	CT-Scan	473 CT Slices for COVID-19	Resizing, GL, Intensity Normalization	Keras	U-Net	50	Sigmoid	Visualization	NA	Dice Score=83.1 Sen=86.7 Spe=99.3
[133]	6 Different Datasets	X-ray	Different Number of Cases	Histogram, Segmentation using U-Net, Intensity Normalization	PyTorch	ResNet18	Standard	Softmax	t-SNE Clustering	NA	Acc=100 Sen=100 Spec=100
[134]	COPD Dataset (Pretrain) COVID-19 Set	CT-Scan	5000 COPDGene, Subjects 470 COVID-19 Subjects	Standard Preprocessing	PyTorch	RTSU-Net	2 RU-Net	Sigmoid, Softmax	Different Methods	NA	IOU=92.2 ASSD=86.6
[135]	Different Dataset	X-ray	180 Images of 118 COVID-19 Subjects, 191 Normal, 54 Bacterial Pneumonia, 57 Tuberculosis, 20 Viral Pneumonia	Standard Preprocessing, Segmentation using FC-DenseNet103	PyTorch	ResNet18	Standard	Majority Voting	Probabilistic Grad-CAM Saliency Map Visualization	NA	Sen=100 Pre=76.9
[136]	COVID-19 Dataset	CT-Scan	60 Patients with COVID-19	Resizing, DA	PyTorch	MiniSeg	Proposed Structure	Sigmoid and Softmax	NA	NA	Sen=83.62 Spe=97.42 DSC=77.28 HD=68.07
[137]	Combination of Different Dataset	X-ray	313 COVID-19 Images, 7595 Normal, 6012 Pneumonia of Unknown Type, 2780 Bacterial Pneumonia Images	Segmentation using U-Net, Standard Preprocessing	NA	VGG-16, VGG-19, Inception-V3	Modified Version	Weighted Average Ensemble Method	Grad-CAM	NA	Acc=99.01 Sen=99.01 Pre=99.01
[138]	COVID-SemiSeg	CT-Scan	100 Labeled Images, 1600 Unlabeled Images of COVID-19	Pseudo Label Generation	PyTorch	Semi-Supervised Inf-Net+Multi-Class Segmentation	Modified Res2Net+ U-Net as Backbones	Sigmoid	NA	NA	Dice=54.1 Sen=56.4 Spe=96.7 MAE=5.7
[139]	Dataset I Dataset II	X-ray	466 Normal, 860 Bacteria, 433 Viruses 210 COVID-19, 330 Others	Adaptive Histogram, CLAHE Method, MoEx, U-Net, DA	NA	Cascade-SEMENet	Modified Version	Sigmoid	Grad-CAM	NA	Acc=85.6 Acc=97.1
[42]	Clinical	CT-Scan	21,658 Images From 861 COVID-19 Patients	Cropping	Pytorch	COVID-SegNet	11 Blocks	Softmax	NA	NA	DSC=72.6 Sen=75.1 Pre=72.6
[140]	Clinical	CT-Scan	10 Axial Volumetric CT-Scans of COVID-19 Pneumonia Patients	Under-Sampling of the Majority Class	Keras with TensorFlow Backend	FCN-8s	NA	NA	NA	NA	Acc=100 Pre=98
[141]	Combination of Different Dataset	CT-Scan	449 COVID-19 Patients, 100 Normal, 98 Lung Cancer, 397 Other Pathology	Resizing, Intensity Normalization	Keras with TensorFlow Backend	Encoder and Two Decoders (2D U-NET) and MLP	24, 24, 15	Sigmoid	NA	NA	Acc=86 Sen=94 Spe=79
[142]	Clinical	CT-Scan	313 COVID-19, 229 Non-COVID-19	Normalizing, Resampling, DA, 3D Lung Mask Generation using 2D U-Net	PyTorch	DeCoVNet	20	Softmax	NA	NA	Acc=90.8
[143]	Clinical	CT-Scan	877 COVID-19, 991 Non-COVID-19	Visual Data Annotation and Quality, Normalization, 3D U-Net++ for Segmentation, DA	PyTorch	ResNet50	Standard Version	Softmax	NA	NA	Sen=97.4 Spe=92.2 AUC=99.1
[144]	Clinical	CT-Scan	1315 COVID-19 Scans, 3342 Non-COVID-19 Scans	Lobe Segmentation using 3D-Unet, Cropping, Resizing, DA	Keras with TensorFlow Backend	3D-ResNets with Prior-Attention Mechanism	Modified Version	Softmax	Heatmap Visualization	5	Acc=93.3 Sen=87.6 Spe=95.5
[145]	Clinical	LUS Images	17 COVID-19 Patients, 4 Were COVID-19 Suspected, and 14 Were Healthy	Labelling Process, DA, Reg-STN Model	NA	CNN	NA	Loss Function	Segmentation	5	NA
[146]	Clinical	CT-Scan	296 COVID-19 Images, 1735 CAP, 1325 Non-Pneumonia Images	Lung Segmentation using U-net	NA	COVNet	Modified Version	Softmax	Grad-CAM	NA	AUC=96 Sen=90 Spe=96
[147]	Clinical	CT-Scan	129 COVID-19 images	Segmentation Using U-Net, Different Preprocessing Methods	NA	ResNet18	Modified Version	Softmax	Calculate the Proportion of Infected Regions in Lung	NA	Acc=93.8 AUC=91.3 m-Dice=74.3
[148]	Clinical	CT-Scan	100 COVID-19 and 100 healthy controls	IDRL Landmarks, DI2IN Segmentation, Alignment, Resampling	Pytorch	DenseUNet	Modified Version	Softmax	Visualization	NA	Different Parameters
[149]	Clinical	CT-Scan	558 COVID-19 Patients	2D CNNs for the Segmentation	PyTorch	Student COPLE-Net+ EMA for Adaptive teacher+ Teacher COPLE-Net	Proposed Architecture	NA	Proposed Loss Function	NA	Dice=80.72 RVE=15.96
[150]	Combination of Different Datasets	CT-Scan	33 COVID-19 Patients, 32 Healthy Patients, 36 Patients with Other Lung Pathologies	Rescaling, Intensity Normalization, Creating Feature Map using U-Net	NA	Different Architectures	NA	NA	NA	3	AUC=95.1 Spearman Correlation=98

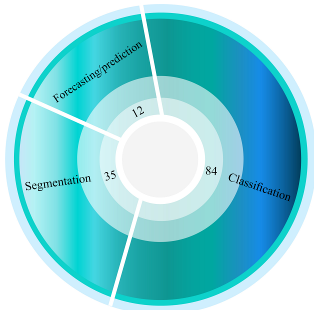

Fig. 7: Total number of investigations conducted in the field of classification, segmentation, and prediction of COVID-19 patients using DL techniques.

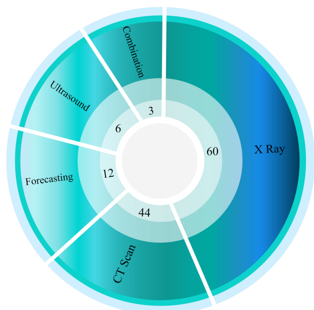

Fig. 8: Number of datasets used for COVID-19 detection and prediction based on the published papers using DL methods.

Fig. 9: Number of DL architectures used for COVID-19 detection and prediction based on published papers.

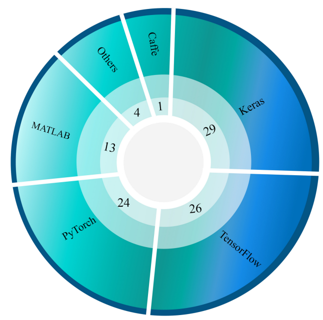

Fig. 10: Number of DL tools used for COVID-19 detection and prediction based on the published papers.

The X-ray, ultrasound, and CT modalities have been used to develop DL models. Figure 8 shows the total number of times each modality is used in reviewed studies. It can be observed that most of the researchers have used X-ray images. This may be due to cheaper registration fees, and the fact that slice selection is not needed. Also, very few research papers have used combined modalities of X-ray and CT images due to the absence of such a comprehensive database.

Various DL models developed for the automated detection of COVID-19 patients are shown in Figure 9. It can be noted from the figure that; different types of convolutional networks have been commonly used. Also, for the automated segmentation of lungs, various types of U-Net are more common.

Nowadays, a variety of toolboxes have been used to implement DL models. The number of toolboxes used for automated detection of COVID-19 by researchers is shown in Figure 10. It can be noted that the Keras toolbox is the most widely used in reviewed papers; this can be due to its simplicity and also the availability of pre-trained models in this library, which are also used frequently by researchers.

The last part of this study is devoted to the classification algorithms developed using DL architectures. The softmax is most employed for automated detection of COVID-19 patients (Tables III to V). Figure 11 shows the number of various classification algorithms used for automated detection of COVID-19 patients using DL techniques.

VI. Challenges

With the rapid growth and spread of COVID-19 globally, researchers have confronted many serious challenges in designing and implementing CADS to diagnose and also forecast the spread of the disease. The most significant challenges associated with COVID-19 are data availability, DL networks architecture fixing, and hardware resources. Lack of availability of a huge public database comprising X-ray and CT images is the first challenge. Due to the limited number of patient data, many researchers have used pre-trained networks such as GoogLeNet and AlexNet. Nevertheless, the number of studies conducted on forecasting is limited as it also requires a vast database.

One of the problems of employing pre-trained networks is that these models are often trained on the ImageNet database, which is entirely different from medical images. Hence, implementing efficient CADS to accurately and swiftly diagnose COVID-19 from X-Ray or CT images is still a challenging work. Physicians are not just convinced with X-ray or CT-scan images of patients to accurately diagnose COVID-19; they may use both modalities simultaneously. However, complete and comprehensive databases of the X-ray and CT-scan hybrid modalities for CADS research and implementation have not been provided for researchers in the machine learning scope. For this reason, researchers combine different X-ray and CT-Scan datasets from various datasets, which may disrupt network training. Yielding the combined X-Ray and CT-Scan datasets pave the path to help quickly identify COVID-19 alongside DL networks. The third challenge in the data section

TABLE V: Summary of DL models developed for the forecasting spread of COVID-19.

Work	Dataset	Preprocessing	DNN Toolbox	DNN	Number of layers	K-Fold	Post Processing	Performance Criteria
[151]	Johns Hopkins University and Canadian Health Authority	WT, ADF test	NA	LSTM	3	NA	NA	RMSE=45.70 Acc=92.67%
[152]	Surging News Network (a Media Outlet) and WHO	Reshaping	NA	CNN	7	NA	NA	MAE=102.943 RMSE=109.439
[153]	Google Trends Website	NA	Keras with Tensor-Flow Backend	LSTM	3	10	NA	RMSE=27.187
[154]	India Government	NA	MATLAB	LSTM	NA	NA	NA	Curves
[155]	Times Series Dataset of COVID-19 Confirmed Cases for Tunisia and China	Grid Search Technique, Sliding Window (SW)	NA	Stacked Ensemble Meta-Learners	DNN: 5 LSTM:5 CNN: 7	NA	Augmented Prediction	Acc=99% RMSE=2,396
[156]	Cumulative and New Confirmed Cases of Covid-19 in All of China and 31 Provinces/ Cities in Mainland and Three Other Regions (Hong Kong, Macau and Taiwan)	Windowing, Normalizing	NA	Modified Auto-Encoders (MAE)	3	5	k-Means	Curves
[157]	COVID-19 Confirmed Data from Iran Ministry of Health and Medical Education, IRNA, ISNA Sources in Provincial Level and National Level	NA	TensorFlow	LSTM	NA	NA	NA	Curves
[158]	Combined of Local Trend Data and Weather Data	Feature Selection using OLS Regression, Network Hyper-Parameters Search	NA	LSTM	3	NA	Fuzzy Rule-Based Risk Categorization	RMSE=2300.8 Acc=78% Curves
[159]	WHO and Johns Hopkins University Datasets	Normalizing	NA	LSTM	4	NA	RMSLE	Curves
[160]	Johns Hopkins University, Lockdown dates of Countries Datasets	Windowing, Normalization, Proposed Improved Method	NA	LSTM	4	NA	NA	Curves
[161]	John Hopkins University, Oxford COVID-19 Government Response Tracker	Feature Selection, Spatially Weighted Adjacency Matrix Computation, Reshaping to 3D Tensor	NA	Variational LSTM-Autoencoder with Self-Attention Mechanism	3 Blocks	NA	NA	Curves
[162]	TheMinistry of Health and Family Welfare (Government of India)	Linear Weighted Moving Average Technique	Keras with Tensor-Flow Backend	Bi-LSTM	3	NA	NA	MAPE Less Than 3%

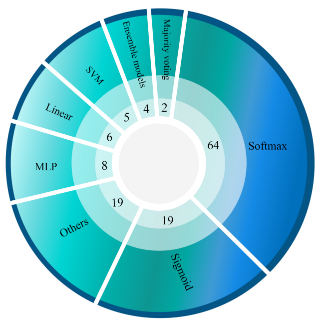

Fig. 11: Illustration of number of various classifier algorithms used in DL networks for automated detection of COVID-19 patients.

is the non-reporting of phenotypic information, such as age and gender. The utilization of this information can amend and enhance the performance of DL algorithms.

Table IV summarizes the DL-based segmentation algorithms aimed at identifying areas suspected of COVID-19 in the X-ray and CT-scan images. One of the obstacles with databases is the absence of manual or ground truths for COVID-19 image segmentation areas. Therefore, many researchers have delineated these areas with the help of radiologists and trained the models such as U-Net, which is time-consuming. Consequently, the presence of dedicated databases of segmented images will help to get the best-performing model. Also, it becomes easy to compare the performances with other authors who have worked on the same images.

In order to predict the prevalence of corona using DL methods, the nature of the COVID-19 is still relatively unknown, and the probability of mutation is a big issue. Therefore, to predict the prevalence of the disease, many factors like the average age of the society, policies to impede the spread of the disease by countries, climatic conditions, and infection of neighbor/friend/family member.

Lack of access to appropriate hardware resources is another challenge. Implementing DL architectures in CADS for corona diagnosis demands strong hardware resources, which unfortunately is not ordinarily accessible for many researchers. Although tools such as Google Colab have partially obviated this problem, employing these tools in real medical applications is still challenging. For this reason, in most studies, researchers have not provided practical CADS systems such as web or Windows software to detect COVID-19.

VII. Conclusion and Future Works

COVID-19 is an emerging pandemic disease that, in a short period of time, can severely endanger the health of many people throughout the world. It directly affects the lung cells, and if not accurately diagnosed early, can cause irreversible damage, including death. The disease is accurately detected by the specialists using X-ray, CT and ultrasound images together with RT-PCR results. Specialized physicians use RT-PCR as the gold standard for COVID-19 diagnosis based on WHO guidelines. The accurate diagnosis of COVID-19 is made using medical imaging methods, including X-Ray, CT, and Ultrasound beside RT-PCR. COVID-19 diagnosis by medical imaging always has some challenges for physicians. The high number of medical images associated with each patient, doctor's fatigue, and low contrast of the images are among some problems challenging the COVID-19 accurate diagnosis. The accurate diagnosis of COVID-19 has high importance, and lack of fast and accurate diagnosis can cause severe damages such as death.

To address this problem, researchers are working on some advanced DL techniques to diagnose COVID-19 accurately in the shortest possible time. In this study, a comprehensive review of the accomplished studies of COVID-19 diagnosis was carried out using DL networks. Frist, the public databases available to detection and prediction of COVID-19 are presented. In the following, the state-of-art DL techniques employed for the diagnosis, segmentation, and forecasting of the spread of COVID-19 are presented in Tables III, IV, V, respectively.

In another section of the paper, some advanced DL methods such as attentions [46], transformers [47], fusion [48], and graph [49] have been introduced. In this section, an introduction to the method has been presented first, then COVID-19 diagnosis papers based on these methods are introduced. In the following, important information of each paper, including various types of DL research for COVID-19 (classifications, segmentation, and predictions), have been explored and compared. In the following, the number of modalities used in

COVID-19 diagnosis, DL models, DL toolboxes, and classification algorithms are introduced.

The most critical challenge of COVID-19 diagnosis using DL techniques is mentioned in section 4. As mentioned, the most critical challenges of COVID-19 diagnosis are dataset, software, and hardware. One of the challenges to develop a robust and accurate COVID 19 diagnosis system is the availability of an extensive public database. We strongly feel that, with more public databases, better DL models can be developed by researchers to detection and prediction of the COVID19 accurately.

Recently, using fusion techniques such as feature fusion has had many improvements in medical applications [163]. In future works, it is possible to use deep feature fusion techniques besides medical imaging modalities to diagnose COVID-19. In addition to that, it is possible to use some advanced DL methods such as zero-shot learning in order to diagnose COVID-19 [164]. In a section of the paper, there were some discussions about attention and transformer techniques. As it is mentioned, each of these methods has a lot of different techniques [165]. So, various attention and transformer models can diagnose COVID-19 in future works.

REFERENCES

[1] J. F.-W. Chan, S. Yuan, K.-H. Kok, K. K.-W. To, H. Chu, J. Yang, F. Xing, J. Liu, C. C.-Y. Yip, R. W.-S. Poon *et al.*, "A familial cluster of pneumonia associated with the 2019 novel coronavirus indicating person-to-person transmission: a study of a family cluster," *The Lancet*, vol. 395, no. 10223, pp. 514–523, 2020.

[2] N. Ghassemi, A. Shoeibi, M. Khodatars, J. Heras, A. Rahimi, A. Zare, R. B. Pachori, and J. M. Gorriz, "Automatic diagnosis of covid-19 from ct images using cyclegan and transfer learning," *arXiv preprint arXiv:2104.11949*, 2021.

[3] J. Lopez Bernal, N. Andrews, C. Gower, E. Gallagher, R. Simmons, S. Thelwall, J. Stowe, E. Tessier, N. Groves, G. Dabrera *et al.*, "Effectiveness of covid-19 vaccines against the b. 1.617. 2 (delta) variant." *N Engl J Med*, pp. 585–594, 2021.

[4] X. Peng, X. Xu, Y. Li, L. Cheng, X. Zhou, and B. Ren, "Transmission routes of 2019-ncov and controls in dental practice," *International Journal of Oral Science*, vol. 12, no. 1, pp. 1–6, 2020.

[5] S. Tian, W. Hu, L. Niu, H. Liu, H. Xu, and S.-Y. Xiao, "Pulmonary pathology of early phase 2019 novel coronavirus (covid-19) pneumonia in two patients with lung cancer," *Journal of Thoracic Oncology*, 2020.

[6] T. C. Lan, M. F. Allan, L. Malsick, S. Khandwala, S. S. Nyeo, M. Bathe, A. Griffiths, and S. Rouskin, "Structure of the full sars-cov-2 rna genome in infected cells," *bioRxiv*, 2020.

[7] A. Remuzzi and G. Remuzzi, "Covid-19 and italy: what next?" *The Lancet*, 2020.

[8] C. Sohrabi, Z. Alsafi, N. O'Neill, M. Khan, A. Kerwan, A. Al-Jabir, C. Iosifidis, and R. Agha, "World health organization declares global emergency: A review of the 2019 novel coronavirus (covid-19)," *International Journal of Surgery*, 2020.

[9] "https://www.ecdc.europa.eu/en/geographical-distribution-2019-ncov-cases," https://www.ecdc.europa.eu/en/geographical-distribution-2019-ncov-cases, 2020.

[10] F. J. P. Montalbo, "Diagnosing covid-19 chest x-rays with a lightweight truncated densenet with partial layer freezing and feature fusion," *Biomedical Signal Processing and Control*, vol. 68, p. 102583, 2021.

[11] D. Singh, V. Kumar, and M. Kaur, "Densely connected convolutional networks-based covid-19 screening model," *Applied Intelligence*, vol. 51, no. 5, pp. 3044–3051, 2021.

[12] W. H. Self, D. M. Courtney, C. D. McNaughton, R. G. Wunderink, and J. A. Kline, "High discordance of chest x-ray and computed tomography for detection of pulmonary opacities in ed patients: implications for diagnosing pneumonia," *The American journal of emergency medicine*, vol. 31, no. 2, pp. 401–405, 2013.

[13] G. D. Rubin, C. J. Ryerson, L. B. Haramati, N. Sverzellati, J. P. Kanne, S. Raoof, N. W. Schluger, A. Volpi, J.-J. Yim, I. B. Martin *et al.*, "The role of chest imaging in patient management during the covid-19 pandemic: a multinational consensus statement from the fleischner society," *Chest*, 2020.

[14] E.-S. M. El-Kenawy, S. Mirjalili, A. Ibrahim, M. Alrahmawy, M. El-Said, R. M. Zaki, and M. M. Eid, "Advanced meta-heuristics, convolutional neural networks, and feature selectors for efficient covid-19 x-ray chest image classification," *IEEE Access*, vol. 9, pp. 36 019–36 037, 2021.

[15] B. Barros, P. Lacerda, C. Albuquerque, and A. Conci, "Pulmonary covid-19: Learning spatiotemporal features combining cnn and lstm networks for lung ultrasound video classification," *Sensors*, vol. 21, no. 16, p. 5486, 2021.

[16] N. Ghassemi, A. Shoeibi, and M. Rouhani, "Deep neural network with generative adversarial networks pre-training for brain tumor classification based on mr images," *Biomedical Signal Processing and Control*, vol. 57, p. 101678, 2020.

[17] M. Talo, O. Yildirim, U. B. Baloglu, G. Aydin, and U. R. Acharya, "Convolutional neural networks for multi-class brain disease detection using mri images," *Computerized Medical Imaging and Graphics*, vol. 78, p. 101673, 2019.

[18] N. Ghassemi, A. Shoeibi, M. Rouhani, and H. Hosseini-Nejad, "Epileptic seizures detection in eeg signals using tqwt and ensemble learning," in *2019 9th International Conference on Computer and Knowledge Engineering (ICCKE)*. IEEE, 2019, pp. 403–408.

[19] M. Mohammadpoor, A. Shoeibi, H. Zare, and H. Shojaee, "A hierarchical classification method for breast tumor detection," *Iranian Journal of Medical Physics*, vol. 13, no. 4, pp. 261–268, 2016.

[20] D. Arefan, A. A. Mohamed, W. A. Berg, M. L. Zuley, J. H. Sumkin, and S. Wu, "Deep learning modeling using normal mammograms for predicting breast cancer risk," *Medical physics*, vol. 47, no. 1, pp. 110–118, 2020.

[21] A. Esteva, B. Kuprel, R. A. Novoa, J. Ko, S. M. Swetter, H. M. Blau, and S. Thrun, "Dermatologist-level classification of skin cancer with deep neural networks," *nature*, vol. 542, no. 7639, pp. 115–118, 2017.

[22] M. A. Mazurowski, M. Buda, A. Saha, and M. R. Bashir, "Deep learning in radiology: An overview of the concepts and a survey of the state of the art with focus on mri," *Journal of magnetic resonance imaging*, vol. 49, no. 4, pp. 939–954, 2019.

[23] T. M. Tuan, T. T. Ngan, C. N. Giap *et al.*, "Semisupervised fuzzy clustering methods for x-ray image segmentation," in *Handbook of Data Science Approaches for Biomedical Engineering*. Elsevier, 2020, pp. 251–289.

[24] A. Shoeibi, N. Ghassemi, H. Hosseini-Nejad, and M. Rouhani, "An efficient brain mr images segmentation hardware using kernel fuzzy c-means," in *2019 26th National and 4th International Iranian Conference on Biomedical Engineering (ICBME)*. IEEE, 2019, pp. 93–99.

[25] O. Ronneberger, P. Fischer, and T. Brox, "U-net: Convolutional networks for biomedical image segmentation," in *International Conference on Medical image computing and computer-assisted intervention*. Springer, 2015, pp. 234–241.

[26] J. P. Cohen, P. Morrison, L. Dao, K. Roth, T. Q. Duong, and M. Ghassemi, "Covid-19 image data collection: Prospective predictions are the future," *arXiv 2006.11988*, 2020. [Online]. Available: https://github.com/ieee8023/covid-chestxray-dataset

[27] J. Zhao, Y. Zhang, X. He, and P. Xie, "Covid-ct-dataset: a ct scan dataset about covid-19," *arXiv preprint arXiv:2003.13865*, 2020.

[28] J. Born, G. Brändle, M. Cossio, M. Disdier, J. Goulet, J. Roulin, and N. Wiedemann, "Pocovid-net: Automatic detection of covid-19 from a new lung ultrasound imaging dataset (pocus)," *arXiv preprint arXiv:2004.12084*, 2020.

[29] J. M. Banda, R. Tekumalla, G. Wang, J. Yu, T. Liu, Y. Ding, and G. Chowell, "A large-scale covid-19 twitter chatter dataset for open scientific research–an international collaboration," *arXiv preprint arXiv:2004.03688*, 2020.

[30] R. Hu, G. Ruan, S. Xiang, M. Huang, Q. Liang, and J. Li, "Automated diagnosis of covid-19 using deep learning and data augmentation on chest ct," *medRxiv*, 2020.

[31] Z. Q. L. Linda Wang and A. Wong, "Covid-net: A tailored deep convolutional neural network design for detection of covid-19 cases from chest radiography images," 2020.

[32] Y. Yang, Y. Hu, X. Zhang, and S. Wang, "Two-stage selective ensemble of cnn via deep tree training for medical image classification," *IEEE Transactions on Cybernetics*, 2021.

[33] H. S. Maghdid, A. T. Asaad, K. Z. Ghafoor, A. S. Sadiq, and M. K. Khan, "Diagnosing covid-19 pneumonia from x-ray and ct images

using deep learning and transfer learning algorithms," *arXiv preprint arXiv:2004.00038*, 2020.

[34] Y. Zhou, G. G. Yen, and Z. Yi, "A knee-guided evolutionary algorithm for compressing deep neural networks," *IEEE transactions on cybernetics*, vol. 51, no. 3, pp. 1626–1638, 2019.

[35] M. Loey, F. Smarandache, and N. E. M Khalifa, "Within the lack of chest covid-19 x-ray dataset: A novel detection model based on gan and deep transfer learning," *Symmetry*, vol. 12, no. 4, p. 651, 2020.

[36] M. Ghafoor, S. A. Tariq, T. Zia, I. A. Taj, A. Abbas, A. Hassan, and A. Y. Zomaya, "Fingerprint identification with shallow multifeature view classifier," *IEEE transactions on cybernetics*, 2019.

[37] B. Xiao, Z. Yang, X. Qiu, J. Xiao, G. Wang, W. Zeng, W. Li, Y. Nian, and W. Chen, "Pam-densenet: A deep convolutional neural network for computer-aided covid-19 diagnosis," *IEEE Transactions on Cybernetics*, 2021.

[38] S. Minaee, R. Kafieh, M. Sonka, S. Yazdani, and G. J. Soufi, "Deep-covid: Predicting covid-19 from chest x-ray images using deep transfer learning," *arXiv preprint arXiv:2004.09363*, 2020.

[39] X. Yi, E. Walia, and P. Babyn, "Generative adversarial network in medical imaging: A review," *Medical image analysis*, vol. 58, p. 101552, 2019.

[40] I. Goodfellow, J. Pouget-Abadie, M. Mirza, B. Xu, D. Warde-Farley, S. Ozair, A. Courville, and Y. Bengio, "Generative adversarial nets," in *Advances in neural information processing systems*, 2014, pp. 2672–2680.

[41] D. Nie, L. Wang, E. Adeli, C. Lao, W. Lin, and D. Shen, "3-d fully convolutional networks for multimodal isointense infant brain image segmentation," *IEEE transactions on cybernetics*, vol. 49, no. 3, pp. 1123–1136, 2018.

[42] Q. Yan, B. Wang, D. Gong, C. Luo, W. Zhao, J. Shen, Q. Shi, S. Jin, L. Zhang, and Z. You, "Covid-19 chest ct image segmentation–a deep convolutional neural network solution," *arXiv preprint arXiv:2004.10987*, 2020.

[43] Y.-H. Wu, S.-H. Gao, J. Mei, J. Xu, D.-P. Fan, C.-W. Zhao, and M.-M. Cheng, "Jcs: An explainable covid-19 diagnosis system by joint classification and segmentation," *arXiv preprint arXiv:2004.07054*, 2020.

[44] T. Zhou, S. Canu, and S. Ruan, "An automatic covid-19 ct segmentation network using spatial and channel attention mechanism." *arXiv preprint arXiv:2004.06673*, 2020.

[45] J. Chung, C. Gulcehre, K. Cho, and Y. Bengio, "Empirical evaluation of gated recurrent neural networks on sequence modeling," *arXiv preprint arXiv:1412.3555*, 2014.

[46] C. Sitaula and M. B. Hossain, "Attention-based vgg-16 model for covid-19 chest x-ray image classification," *Applied Intelligence*, vol. 51, no. 5, pp. 2850–2863, 2021.

[47] S. Perera, S. Adhikari, and A. Yilmaz, "Pocformer: A lightweight transformer architecture for detection of covid-19 using point of care ultrasound," *arXiv preprint arXiv:2105.09913*, 2021.

[48] U. Özkaya, Ş. Öztürk, and M. Barstugan, "Coronavirus (covid-19) classification using deep features fusion and ranking technique," in *Big Data Analytics and Artificial Intelligence Against COVID-19: Innovation Vision and Approach*. Springer, 2020, pp. 281–295.

[49] X. Liang, Y. Zhang, J. Wang, Q. Ye, Y. Liu, and J. Tong, "Diagnosis of covid-19 pneumonia based on graph convolutional network," *Frontiers in Medicine*, vol. 7, p. 1071, 2021.

[50] M. Farooq and A. Hafeez, "Covid-resnet: A deep learning framework for screening of covid19 from radiographs," *arXiv preprint arXiv:2003.14395*, 2020.

[51] A. Narin, C. Kaya, and Z. Pamuk, "Automatic detection of coronavirus disease (covid-19) using x-ray images and deep convolutional neural networks," *arXiv preprint arXiv:2003.10849*, 2020.

[52] E. E.-D. Hemdan, M. A. Shouman, and M. E. Karar, "Covidx-net: A framework of deep learning classifiers to diagnose covid-19 in x-ray images," *arXiv preprint arXiv:2003.11055*, 2020.

[53] J. Zhang, Y. Xie, Y. Li, C. Shen, and Y. Xia, "Covid-19 screening on chest x-ray images using deep learning based anomaly detection," *arXiv preprint arXiv:2003.12338*, 2020.

[54] X. Qi, L. G. Brown, D. J. Foran, J. Nosher, and I. Hacihaliloglu, "Chest x-ray image phase features for improved diagnosis of covid-19 using convolutional neural network," *International journal of computer assisted radiology and surgery*, vol. 16, no. 2, pp. 197–206, 2021.

[55] F. Ucar and D. Korkmaz, "Covidiagnosis-net: Deep bayes-squeezenet based diagnostic of the coronavirus disease 2019 (covid-19) from x-ray images," *Medical Hypotheses*, p. 109761, 2020.

[56] B. Ghoshal and A. Tucker, "Estimating uncertainty and interpretability in deep learning for coronavirus (covid-19) detection," *arXiv preprint arXiv:2003.10769*, 2020.

[57] M. Toğaçar, B. Ergen, and Z. Cömert, "Covid-19 detection using deep learning models to exploit social mimic optimization and structured chest x-ray images using fuzzy color and stacking approaches," *Computers in Biology and Medicine*, p. 103805, 2020.

[58] X. Wu, H. Hui, M. Niu, L. Li, L. Wang, B. He, X. Yang, L. Li, H. Li, J. Tian *et al.*, "Deep learning-based multi-view fusion model for screening 2019 novel coronavirus pneumonia: a multicentre study," *European Journal of Radiology*, p. 109041, 2020.

[59] A. A. Ardakani, A. R. Kanafi, U. R. Acharya, N. Khadem, and A. Mohammadi, "Application of deep learning technique to manage covid-19 in routine clinical practice using ct images: Results of 10 convolutional neural networks," *Computers in Biology and Medicine*, p. 103795, 2020.

[60] A. Abbas, M. M. Abdelsamea, and M. M. Gaber, "Classification of covid-19 in chest x-ray images using detrac deep convolutional neural network," *arXiv preprint arXiv:2003.13815*, 2020.

[61] R. M. Pereira, D. Bertolini, L. O. Teixeira, C. N. Silla Jr, and Y. M. Costa, "Covid-19 identification in chest x-ray images on flat and hierarchical classification scenarios," *Computer Methods and Programs in Biomedicine*, p. 105532, 2020.

[62] N. E. M. Khalifa, M. H. N. Taha, A. E. Hassanien, and S. Elghamrawy, "Detection of coronavirus (covid-19) associated pneumonia based on generative adversarial networks and a fine-tuned deep transfer learning model using chest x-ray dataset," *arXiv preprint arXiv:2004.01184*, 2020.

[63] M. Ahsan, M. Based, J. Haider, M. Kowalski *et al.*, "Covid-19 detection from chest x-ray images using feature fusion and deep learning," *Sensors*, vol. 21, no. 4, p. 1480, 2021.

[64] P. Afshar, S. Heidarian, F. Naderkhani, A. Oikonomou, K. N. Plataniotis, and A. Mohammadi, "Covid-caps: A capsule network-based framework for identification of covid-19 cases from x-ray images," *arXiv preprint arXiv:2004.02696*, 2020.

[65] A. I. Khan, J. L. Shah, and M. M. Bhat, "Coronet: A deep neural network for detection and diagnosis of covid-19 from chest x-ray images," *Computer Methods and Programs in Biomedicine*, p. 105581, 2020.

[66] K. Hammoudi, H. Benhabiles, M. Melkemi, F. Dornaika, I. Arganda-Carreras, D. Collard, and A. Scherpereel, "Deep learning on chest x-ray images to detect and evaluate pneumonia cases at the era of covid-19," *arXiv preprint arXiv:2004.03399*, 2020.

[67] E. Luz, P. L. Silva, R. Silva, and G. Moreira, "Towards an efficient deep learning model for covid-19 patterns detection in x-ray images," *arXiv preprint arXiv:2004.05717*, 2020.

[68] M. Karim, T. Döhmen, D. Rebholz-Schuhmann, S. Decker, M. Cochez, O. Beyan *et al.*, "Deepcovidexplainer: Explainable covid-19 predictions based on chest x-ray images," *arXiv preprint arXiv:2004.04582*, 2020.

[69] K. Shankar and E. Perumal, "A novel hand-crafted with deep learning features based fusion model for covid-19 diagnosis and classification using chest x-ray images," *Complex & Intelligent Systems*, vol. 7, no. 3, pp. 1277–1293, 2021.

[70] D. Ezzat, H. A. Ella *et al.*, "Gsa-densenet121-covid-19: a hybrid deep learning architecture for the diagnosis of covid-19 disease based on gravitational search optimization algorithm," *arXiv preprint arXiv:2004.05084*, 2020.

[71] J. de Moura, L. Ramos, P. L. Vidal, M. Cruz, L. Abelairas, E. Castro, J. Novo, and M. Ortega, "Deep convolutional approaches for the analysis of covid-19 using chest x-ray images from portable devices," *medRxiv*, 2020.

[72] F. Ozyurt, T. Tuncer, and A. Subasi, "An automated covid-19 detection based on fused dynamic exemplar pyramid feature extraction and hybrid feature selection using deep learning," *Computers in Biology and Medicine*, vol. 132, p. 104356, 2021.

[73] S. Basu and S. Mitra, "Deep learning for screening covid-19 using chest x-ray images," *arXiv preprint arXiv:2004.10507*, 2020.

[74] M. Rahimzadeh and A. Attar, "A new modified deep convolutional neural network for detecting covid-19 from x-ray images," *arXiv preprint arXiv:2004.08052*, 2020.

[75] Y. Zhang, S. Niu, Z. Qiu, Y. Wei, P. Zhao, J. Yao, J. Huang, Q. Wu, and M. Tan, "Covid-da: Deep domain adaptation from typical pneumonia to covid-19," *arXiv preprint arXiv:2005.01577*, 2020.

[76] M. Ramadhan, A. Faza, L. Lubis, R. Yunus, T. Salamah, D. Handayani, I. Lestariningsih, A. Resa, C. Alam, P. Prajitno *et al.*, "Fast and accurate detection of covid-19-related pneumonia from chest x-ray images with novel deep learning model," *arXiv preprint arXiv:2005.04562*, 2020.

[77] S. Tang, C. Wang, J. Nie, N. Kumar, Y. Zhang, Z. Xiong, and A. Barnawi, "Edl-covid: Ensemble deep learning for covid-19 cases detection from chest x-ray images," *IEEE Transactions on Industrial Informatics*, 2021.

[78] Y. Song, S. Zheng, L. Li, X. Zhang, X. Zhang, Z. Huang, J. Chen, H. Zhao, Y. Jie, R. Wang *et al.*, "Deep learning enables accurate diagnosis of novel coronavirus (covid-19) with ct images," *medRxiv*, 2020.

[79] S. Wang, D. Dong, L. Li, H. Li, Y. Bai, Y. Hu, Y. Huang, X. Yu, S. Liu, X. Qiu *et al.*, "A deep learning radiomics model to identify poor outcome in covid-19 patients with underlying health conditions: a multicenter study," *IEEE Journal of Biomedical and Health Informatics*, 2021.

[80] I. Razzak, S. Naz, A. Rehman, A. Khan, and A. Zaib, "Improving coronavirus (covid-19) diagnosis using deep transfer learning," *medRxiv*, 2020.

[81] S. Dong, Q. Yang, Y. Fu, M. Tian, and C. Zhuo, "Rconet: Deformable mutual information maximization and high-order uncertainty-aware learning for robust covid-19 detection," *IEEE Transactions on Neural Networks and Learning Systems*, 2021.

[82] S. Rajaraman and S. Antani, "Training deep learning algorithms with weakly labeled pneumonia chest x-ray data for covid-19 detection," *medRxiv*, 2020.

[83] T. Javaheri, M. Homayounfar, Z. Amoozgar, R. Reiazi, F. Homayounieh, E. Abbas, A. Laali, A. R. Radmard, M. H. Gharib, S. A. J. Mousavi *et al.*, "Covidctnet: An open-source deep learning approach to identify covid-19 using ct image," *arXiv preprint arXiv:2005.03059*, 2020.

[84] M. Jamil, I. Hussain *et al.*, "Automatic detection of covid-19 infection from chest x-ray using deep learning," *medRxiv*, 2020.

[85] R. Hu, G. Ruan, S. Xiang, M. Huang, Q. Liang, and J. Li, "Automated diagnosis of covid-19 using deep learning and data augmentation on chest ct," *medRxiv*, 2020.

[86] O. D. T. Catalá, I. S. Igual, F. J. Pérez-Benito, D. M. Escrivá, V. O. Castelló, R. Llobet, and J.-C. Peréz-Cortés, "Bias analysis on public x-ray image datasets of pneumonia and covid-19 patients," *IEEE Access*, vol. 9, pp. 42 370–42 383, 2021.

[87] X. He, X. Yang, S. Zhang, J. Zhao, Y. Zhang, E. Xing, and P. Xie, "Sample-efficient deep learning for covid-19 diagnosis based on ct scans," *medRxiv*, 2020.

[88] X. Ouyang, J. Huo, L. Xia, F. Shan, J. Liu, Z. Mo, F. Yan, Z. Ding, Q. Yang, B. Song *et al.*, "Dual-sampling attention network for diagnosis of covid-19 from community acquired pneumonia," *IEEE Transactions on Medical Imaging*, 2020.

[89] L. Sarker, M. Islam, T. Hannan, and A. Zakaria, "Covid-densenet: A deep learning architecture to detect covid-19 from chest radiology images," *Preprints*, 2020.

[90] S. Yang, L. Jiang, Z. Cao, L. Wang, J. Cao, R. Feng, Z. Zhang, X. Xue, Y. Shi, and F. Shan, "Deep learning for detecting corona virus disease 2019 (covid-19) on high-resolution computed tomography: a pilot study," *Annals of Translational Medicine*, vol. 8, no. 7, 2020.

[91] P. K. Sethy and S. K. Behera, "Detection of coronavirus disease (covid-19) based on deep features," *Preprints*, vol. 2020030300, p. 2020, 2020.

[92] I. D. Apostolopoulos, S. I. Aznaouridis, and M. A. Tzani, "Extracting possibly representative covid-19 biomarkers from x-ray images with deep learning approach and image data related to pulmonary diseases," *Journal of Medical and Biological Engineering*, p. 1, 2020.

[93] A. Waheed, M. Goyal, D. Gupta, A. Khanna, F. Al-Turjman, and P. R. Pinheiro, "Covidgan: Data augmentation using auxiliary classifier gan for improved covid-19 detection," *IEEE Access*, vol. 8, pp. 91 916–91 923, 2020.

[94] G. Wang, X. Liu, C. Li, Z. Xu, J. Ruan, H. Zhu, T. Meng, K. Li, N. Huang, and S. Zhang, "A noise-robust framework for automatic segmentation of covid-19 pneumonia lesions from ct images," *IEEE Transactions on Medical Imaging*, vol. 39, no. 8, pp. 2653–2663, 2020.

[95] A. M. Hasan, M. M. AL-Jawad, H. A. Jalab, H. Shaiba, R. W. Ibrahim, and A. R. AL-Shamasneh, "Classification of covid-19 coronavirus, pneumonia and healthy lungs in ct scans using q-deformed entropy and deep learning features," *Entropy*, vol. 22, no. 5, p. 517, 2020.

[96] I. D. Apostolopoulos and T. A. Mpesiana, "Covid-19: automatic detection from x-ray images utilizing transfer learning with convolutional neural networks," *Physical and Engineering Sciences in Medicine*, p. 1, 2020.

[97] P. R. Bassi and R. Attux, "A deep convolutional neural network for covid-19 detection using chest x-rays," *arXiv preprint arXiv:2005.01578*, 2020.

[98] J. P. Cohen, L. Dao, P. Morrison, K. Roth, Y. Bengio, B. Shen, A. Abbasi, M. Hoshmand-Kochi, M. Ghassemi, H. Li *et al.*, "Predicting covid-19 pneumonia severity on chest x-ray with deep learning," *arXiv preprint arXiv:2005.11856*, 2020.

[99] M. E. Chowdhury, T. Rahman, A. Khandakar, R. Mazhar, M. A. Kadir, Z. B. Mahbub, K. R. Islam, M. S. Khan, A. Iqbal, N. Al-Emadi *et al.*, "Can ai help in screening viral and covid-19 pneumonia?" *arXiv preprint arXiv:2003.13145*, 2020.

[100] M. Loey, G. Manogaran, and N. E. M. Khalifa, "A deep transfer learning model with classical data augmentation and cgan to detect covid-19 from chest ct radiography digital images," 2020.

[101] M. Rahimzadeh and A. Attar, "A modified deep convolutional neural network for detecting covid-19 and pneumonia from chest x-ray images based on the concatenation of xception and resnet50v2," *Informatics in Medicine Unlocked*, p. 100360, 2020.

[102] N. Bansal and S. Sridhar, "Classification of x-ray images for detecting covid-19 using deep transfer learning," 2020.

[103] B. D. Goodwin, C. Jaskolski, C. Zhong, and H. Asmani, "Intra-model variability in covid-19 classification using chest x-ray images," *arXiv preprint arXiv:2005.02167*, 2020.

[104] N. E. M. Khalifa, F. Smarandache, and M. Loey, "A study of the neutrosophic set significance on deep transfer learning models: An experimental case on a limited covid-19 chest x-ray dataset," *Preprints*, 2020.

[105] S. H. Kassani, P. H. Kassasni, M. J. Wesolowski, K. A. Schneider, and R. Deters, "Automatic detection of coronavirus disease (covid-19) in x-ray and ct images: A machine learning-based approach," *arXiv preprint arXiv:2004.10641*, 2020.

[106] S. Vaid, R. Kalantar, and M. Bhandari, "Deep learning covid-19 detection bias: accuracy through artificial intelligence," *International Orthopaedics*, p. 1, 2020.

[107] J. Pu, J. Leader, A. Bandos, J. Shi, P. Du, J. Yu, B. Yang, S. Ke, Y. Guo, J. B. Field *et al.*, "Any unique image biomarkers associated with covid-19?" *European Radiology*, p. 1, 2020.

[108] K. Yang, X. Liu, Y. Yang, X. Liao, R. Wang, X. Zeng, Y. Wang, M. Zhang, and T. Zhang, "End-to-end covid-19 screening with 3d deep learning on chest computed tomography," 2020.

[109] Y. Pathak, P. K. Shukla, A. Tiwari, S. Stalin, S. Singh, and P. K. Shukla, "Deep transfer learning based classification model for covid-19 disease," *IRBM*, 2020.

[110] H. Panwar, P. Gupta, M. K. Siddiqui, R. Morales-Menendez, and V. Singh, "Application of deep learning for fast detection of covid-19 in x-rays using ncovnet," *Chaos, Solitons & Fractals*, p. 109944, 2020.

[111] M. A. Al-antari, C.-H. Hua, and S. Lee, "Fast deep learning computer-aided diagnosis against the novel covid-19 pandemic from digital chest x-ray images," 2020.

[112] L. Brunese, F. Mercaldo, A. Reginelli, and A. Santone, "Explainable deep learning for pulmonary disease and coronavirus covid-19 detection from x-rays," *Computer Methods and Programs in Biomedicine*, p. 105608, 2020.

[113] X. Li, C. Li, and D. Zhu, "Covid-mobilexpert: On-device covid-19 screening using snapshots of chest x-ray," *arXiv preprint arXiv:2004.03042*, 2020.

[114] D. Singh, V. Kumar, and M. Kaur, "Classification of covid-19 patients from chest ct images using multi-objective differential evolution–based convolutional neural networks," *European Journal of Clinical Microbiology & Infectious Diseases*, pp. 1–11, 2020.

[115] J. Diaz-Escobar, N. E. Ordóñez-Guillén, S. Villarreal-Reyes, A. Galaviz-Mosqueda, V. Kober, R. Rivera-Rodriguez, and J. E. Lozano Rizk, "Deep-learning based detection of covid-19 using lung ultrasound imagery," *Plos one*, vol. 16, no. 8, p. e0255886, 2021.

[116] J. Song, H. Wang, Y. Liu, W. Wu, G. Dai, Z. Wu, P. Zhu, W. Zhang, K. W. Yeom, and K. Deng, "End-to-end automatic differentiation of the coronavirus disease 2019 (covid-19) from viral pneumonia based on chest ct," *European journal of nuclear medicine and molecular imaging*, pp. 1–9, 2020.

[117] S. E. Ebadi, D. Krishnaswamy, S. E. S. Bolouri, D. Zonoobi, R. Greiner, N. Meuser-Herr, J. L. Jaremko, J. Kapur, M. Noga, and K. Punithakumar, "Automated detection of pneumonia in lung ultrasound using deep video classification for covid-19," *Informatics in Medicine Unlocked*, vol. 25, p. 100687, 2021.

[118] A. Saeedi, M. Saeedi, and A. Maghsoudi, "A novel and reliable deep learning web-based tool to detect covid-19 infection form chest ct-scan," *arXiv preprint arXiv:2006.14419*, 2020.

[119] P. R. Bassi and R. Attux, "A deep convolutional neural network for covid-19 detection using chest x-rays," *arXiv preprint arXiv:2005.01578*, 2020.

[120] M. Siddhartha and A. Santra, "Covidlite: A depth-wise separable deep neural network with white balance and clahe for detection of covid-19," *arXiv preprint arXiv:2006.13873*, 2020.

[121] N. Awasthi, A. Dayal, L. R. Cenkeramaddi, and P. K. Yalavarthy, "Mini-covidnet: Efficient lightweight deep neural network for ultrasound based point-of-care detection of covid-19," *IEEE Transactions on Ultrasonics, Ferroelectrics, and Frequency Control*, vol. 68, no. 6, pp. 2023–2037, 2021.

[122] P. G. Moutounet-Cartan, "Deep convolutional neural networks to diagnose covid-19 and other pneumonia diseases from posteroanterior chest x-rays," *arXiv preprint arXiv:2005.00845*, 2020.

[123] H. Hirano, K. Koga, and K. Takemoto, "Vulnerability of deep neural networks for detecting covid-19 cases from chest x-ray images to universal adversarial attacks," *arXiv preprint arXiv:2005.11061*, 2020.

[124] P. K. Sethy, S. K. Behera, P. K. Ratha, and P. Biswas, "Detection of coronavirus disease (covid-19) based on deep features and support vector machine."

[125] A. Haghanifar, M. M. Majdabadi, and S. Ko, "Covid-cxnet: Detecting covid-19 in frontal chest x-ray images using deep learning," *arXiv preprint arXiv:2006.13807*, 2020.

[126] M. La Salvia, G. Secco, E. Torti, G. Florimbi, L. Guido, P. Lago, F. Salinaro, S. Perlini, and F. Leporati, "Deep learning and lung ultrasound for covid-19 pneumonia detection and severity classification," *Computers in Biology and Medicine*, vol. 136, p. 104742, 2021.

[127] O. Gozes, M. Frid-Adar, H. Greenspan, P. D. Browning, H. Zhang, W. Ji, A. Bernheim, and E. Siegel, "Rapid ai development cycle for the coronavirus (covid-19) pandemic: Initial results for automated detection & patient monitoring using deep learning ct image analysis," *arXiv preprint arXiv:2003.05037*, 2020.

[128] F. Shan, Y. Gao, J. Wang, W. Shi, N. Shi, M. Han, Z. Xue, and Y. Shi, "Lung infection quantification of covid-19 in ct images with deep learning," *arXiv preprint arXiv:2003.04655*, 2020.

[129] J. Zhao, Y. Zhang, X. He, and P. Xie, "Covid-ct-dataset: a ct scan dataset about covid-19," *arXiv preprint arXiv:2003.13865*, 2020.

[130] X. Chen, L. Yao, and Y. Zhang, "Residual attention u-net for automated multi-class segmentation of covid-19 chest ct images," *arXiv preprint arXiv:2004.05645*, 2020.

[131] O. Gozes, M. Frid-Adar, N. Sagie, H. Zhang, W. Ji, and H. Greenspan, "Coronavirus detection and analysis on chest ct with deep learning," *arXiv preprint arXiv:2004.02640*, 2020.

[132] T. Zhou, S. Canu, and S. Ruan, "An automatic covid-19 ct segmentation based on u-net with attention mechanism," *arXiv preprint arXiv:2004.06673*, 2020.

[133] E. Tartaglione, C. A. Barbano, C. Berzovini, M. Calandri, and M. Grangetto, "Unveiling covid-19 from chest x-ray with deep learning: a hurdles race with small data," *arXiv preprint arXiv:2004.05405*, 2020.

[134] W. Xie, C. Jacobs, J.-P. Charbonnier, and B. van Ginneken, "Relational modeling for robust and efficient pulmonary lobe segmentation in ct scans," *IEEE Transactions on Medical Imaging*, 2020.

[135] Y. Oh, S. Park, and J. C. Ye, "Deep learning covid-19 features on cxr using limited training data sets," *IEEE Transactions on Medical Imaging*, 2020.

[136] Y. Qiu, Y. Liu, and J. Xu, "Miniseg: An extremely minimum network for efficient covid-19 segmentation," *arXiv preprint arXiv:2004.09750*, 2020.

[137] S. Rajaraman, J. Siegelman, P. O. Alderson, L. S. Folio, L. R. Folio, and S. K. Antani, "Iteratively pruned deep learning ensembles for covid-19 detection in chest x-rays," *arXiv preprint arXiv:2004.08379*, 2020.

[138] D.-P. Fan, T. Zhou, G.-P. Ji, Y. Zhou, G. Chen, H. Fu, J. Shen, and L. Shao, "Inf-net: Automatic covid-19 lung infection segmentation from ct images," *IEEE Transactions on Medical Imaging*, 2020.

[139] D. Lv, W. Qi, Y. Li, L. Sun, and Y. Wang, "A cascade network for detecting covid-19 using chest x-rays," *arXiv preprint arXiv:2005.01468*, 2020.

[140] A. Voulodimos, E. Protopapadakis, I. Katsamenis, A. Doulamis, and N. Doulamis, "Deep learning models for covid-19 infected area segmentation in ct images," *medRxiv*, 2020.

[141] A. Amyar, R. Modzelewski, and S. Ruan, "Multi-task deep learning based ct imaging analysis for covid-19: Classification and segmentation," *medRxiv*, 2020.

[142] C. Zheng, X. Deng, Q. Fu, Q. Zhou, J. Feng, H. Ma, W. Liu, and X. Wang, "Deep learning-based detection for covid-19 from chest ct using weak label," *medRxiv*, 2020.

[143] S. Jin, B. Wang, H. Xu, C. Luo, L. Wei, W. Zhao, X. Hou, W. Ma, Z. Xu, Z. Zheng *et al.*, "Ai-assisted ct imaging analysis for covid-19 screening: Building and deploying a medical ai system in four weeks," *medRxiv*, 2020.

[144] J. Wang, Y. Bao, Y. Wen, H. Lu, H. Luo, Y. Xiang, X. Li, C. Liu, and D. Qian, "Prior-attention residual learning for more discriminative covid-19 screening in ct images," *IEEE Transactions on Medical Imaging*, 2020.

[145] S. Roy, W. Menapace, S. Oei, B. Luijten, E. Fini, C. Saltori, I. Huijben, N. Chennakeshava, F. Mento, A. Sentelli *et al.*, "Deep learning for classification and localization of covid-19 markers in point-of-care lung ultrasound," *IEEE Transactions on Medical Imaging*, 2020.

[146] L. Li, L. Qin, Z. Xu, Y. Yin, X. Wang, B. Kong, J. Bai, Y. Lu, Z. Fang, Q. Song *et al.*, "Artificial intelligence distinguishes covid-19 from community acquired pneumonia on chest ct," *Radiology*, p. 200905, 2020.

[147] W. Wu, Y. Shi, X. Li, Y. Zhou, P. Du, S. Lv, T. Liang, and J. Sheng, "Deep learning to estimate the physical proportion of infected region of lung for covid-19 pneumonia with ct image set," *arXiv preprint arXiv:2006.05018*, 2020.

[148] S. Chaganti, A. Balachandran, G. Chabin, S. Cohen, T. Flohr, B. Georgescu, P. Grenier, S. Grbic, S. Liu, F. Mellot *et al.*, "Quantification of tomographic patterns associated with covid-19 from chest ct," *arXiv preprint arXiv:2004.01279*, 2020.

[149] Z. Han, B. Wei, Y. Hong, T. Li, J. Cong, X. Zhu, H. Wei, and W. Zhang, "Accurate screening of covid-19 using attention based deep 3d multiple instance learning," *IEEE Transactions on Medical Imaging*, 2020.

[150] M. Goncharov, M. Pisov, A. Shevtsov, B. Shirokikh, A. Kurmukov, I. Blokhin, V. Chernina, A. Solovev, V. Gombolevskiy, S. Morozov *et al.*, "Ct-based covid-19 triage: Deep multitask learning improves joint identification and severity quantification," *arXiv preprint arXiv:2006.01441*, 2020.

[151] V. K. R. Chimmula and L. Zhang, "Time series forecasting of covid-19 transmission in canada using lstm networks," *Chaos, Solitons & Fractals*, p. 109864, 2020.

[152] C.-J. Huang and P.-H. Kuo, "Multiple-input deep convolutional neural network model for short-term photovoltaic power forecasting," *IEEE Access*, vol. 7, pp. 74 822–74 834, 2019.

[153] S. M. Ayyoubzadeh, S. M. Ayyoubzadeh, H. Zahedi, M. Ahmadi, and S. R. N. Kalhori, "Predicting covid-19 incidence through analysis of google trends data in iran: data mining and deep learning pilot study," *JMIR Public Health and Surveillance*, vol. 6, no. 2, p. e18828, 2020.

[154] A. Tomar and N. Gupta, "Prediction for the spread of covid-19 in india and effectiveness of preventive measures," *Science of The Total Environment*, p. 138762, 2020.

[155] N. B. Yahia, M. D. Kandara, and N. B. B. Saoud, "Deep ensemble learning method to forecast covid-19 outbreak," 2020.

[156] Z. Hu, Q. Ge, L. Jin, and M. Xiong, "Artificial intelligence forecasting of covid-19 in china," *arXiv preprint arXiv:2002.07112*, 2020.

[157] M. Azarafza, M. Azarafza, and J. Tanha, "Covid-19 infection forecasting based on deep learning in iran," *medRxiv*, 2020.

[158] R. Pal, A. A. Sekh, S. Kar, and D. K. Prasad, "Neural network based country wise risk prediction of covid-19," *arXiv preprint arXiv:2004.00959*, 2020.

[159] L. R. Kolozsvari, T. Berczes, A. Hajdu, R. Gesztelyi, A. TIba, I. Varga, G. J. Szollosi, S. Harsanyi, S. Garboczy, and J. Zsuga, "Predicting the epidemic curve of the coronavirus (sars-cov-2) disease (covid-19) using artificial intelligence," *medRxiv*, 2020.

[160] B. Yan, X. Tang, B. Liu, J. Wang, Y. Zhou, G. Zheng, Q. Zou, Y. Lu, and W. Tu, "An improved method of covid-19 case fitting and prediction based on lstm," *arXiv preprint arXiv:2005.03446*, 2020.

[161] M. R. Ibrahim, J. Haworth, A. Lipani, N. Aslam, T. Cheng, and N. Christie, "Variational-lstm autoencoder to forecast the spread of coronavirus across the globe," *medRxiv*, 2020.

[162] P. Arora, H. Kumar, and B. K. Panigrahi, "Prediction and analysis of covid-19 positive cases using deep learning models: A descriptive case study of india," *Chaos, Solitons & Fractals*, p. 110017, 2020.

[163] X. Liu, L. Yang, J. Chen, S. Yu, and K. Li, "Region-to-boundary deep learning model with multi-scale feature fusion for medical image segmentation," *Biomedical Signal Processing and Control*, vol. 71, p. 103165, 2022.

[164] J. Li, M. Jing, K. Lu, L. Zhu, and H. T. Shen, "Investigating the bilateral connections in generative zero-shot learning," *IEEE Transactions on Cybernetics*, 2021.

[165] L. Wu, Y. Wang, X. Li, and J. Gao, "Deep attention-based spatially recursive networks for fine-grained visual recognition," *IEEE transactions on cybernetics*, vol. 49, no. 5, pp. 1791–1802, 2018.